COMPARISON OF SURFACE AREA AND CORTICAL THICKNESS ASYMMETRY IN THE HUMAN AND CHIMPANZEE BRAIN

OXFORD UNIVERSITY PRESS | Cerebral Cortex

COMPARISON OF SURFACE AREA AND CORTICAL THICKNESS ASYMMETRY IN THE HUMAN AND CHIMPANZEE BRAIN

Journal:	*Cerebral Cortex*
Manuscript ID	CerCor-2019-00880.R1
Manuscript Type:	Original Article
Date Submitted by the Author:	01-Jun-2020
Complete List of Authors:	Li, Xiang; University of Edinburgh, Clinical Research Imaging Centre Crow, Tim; SANE POWIC, University Department of Psychiatry Hopkins, William D.; Georgia State University, Neuroscience Institute and Language Research Center Roberts, Neil; University of Edinburgh, Division of Medical and Radiological Sciences
Keywords:	brain asymmetry, chimpanzee, surface area, cortical thickness, species difference

COMPARISON OF SURFACE AREA AND CORTICAL THICKNESS ASYMMETRY IN THE HUMAN AND CHIMPANZEE BRAIN

Li Xiang[a], Timothy J. Crow[b], William D. Hopkins[c], Neil Roberts[a*]

[a] School of Clinical Sciences, University of Edinburgh, EH16 4TJ, United Kingdom

[b] POWIC, University Department of Psychiatry, Warneford Hospital, Oxford, OX3 7JX, United Kingdom

[c] The University of Texas MD Anderson Cancer Centre, Bastrop, Texas 78602, United States

Corresponding Author:
Neil Roberts
School of Clinical Sciences
University of Edinburgh
EH16 4TJ
United Kingdom
neil.roberts@ed.ac.uk

Abstract

Which structural asymmetries underpin the lateralization of the human brain function can be clarified by comparison with chimpanzees. Here we report the results of vertex-wise and ROI-based analyses that compared surface area (SA) and cortical thickness (CT) asymmetries in 3D MR images obtained for 91 humans and 77 chimpanzees. We find that the human brain has substantially greater asymmetry than the chimpanzee's. Specially, there is (i) larger total SA in the right compared to the left cerebral hemisphere, (ii) a global asymmetry pattern of widespread thicker cortex in the left compared to the right frontal and the right compared to the left temporo-parieto-occipital lobe and (iii) local asymmetries, most notably in the superior temporal sulcus and medial occipital cortex where rightward asymmetry is observed for both SA and CT. There is also (iv) a prominent asymmetry specific to the chimpanzee brain, namely the rightward CT asymmetry in the precentral cortex. These findings provide evidence of there being substantial differences in the asymmetry between the human and chimpanzee brain. The unique asymmetries of the human brain are potential neural substrates for cognitive specializations and the presence of significant asymmetry of precentral gyrus in the chimpanzee brain should be further investigated.

Key words: brain asymmetry, chimpanzee, cortical thickness, surface area.

1. Introduction

A key feature of the human brain is the population-level functional and structural asymmetry. Clinical and experimental data obtained using a variety of methods have documented the left hemispheric specializations for linguistic and praxis functions (Knecht et al., 2000; Ocklenburg & Gunturkun, 2018). Several structural asymmetries have been identified in the human brain and are potential neural substrates for the functional lateralization (e.g., Barrick, Lawes, Mackay, & Clark, 2007; Josse, Kherif, Flandin, Seghier, & Price, 2009). For example, the Sylvian fissure typically rises more steeply in the right cerebral hemisphere and extends further posteriorly in the left cerebral hemisphere (Cunningham, 1892; Eberstaller, 1884, 1890; Ide, Rodriguez, Zaidel, & Aboitiz, 1996; Rubens, Mahowald, & Hutton, 1976; Yeni-Komshian & Benson, 1976), and the planum temporale (PT), which is the flat surface of the posterior superior temporal gyrus posterior to Heschl's gyrus, is larger on the left compared to the right in a statistical majority of humans (Geschwind & Levitsky, 1968; Shapleske, Rossell, Woodruff, & David, 1999; Vadlamudi et al., 2006; Witelson & Kigar, 1988). Also notable in the human brain is the so-called torque whereby there is a global anti-clockwise twist in the transverse plane. Its exaggerated posterior component in terms of the protrusion and rightward bending of the left occipital lobe (LeMay, 1982; Witelson and Kigar, 1988; Xiang et al., 2018) is potentially related to the greater posterior extension of the lateral ventricle in the left compared to the right cerebral hemisphere (Narr et al., 2001). A list of brain structural asymmetry studies is provided in Table 1, however, in no means to be comprehensive. Historically, asymmetries in brain structure, cognitive and motor functions have been considered uniquely human and presumed to be evolved after the split from the common ancestor of humans and great apes (Bradshaw & Rogers, 1993; Corballis, 1992; Corballis, 2002; Crow, 2009). However, research over the past 20 to 25 years has challenged this long held view with a growing body of evidence demonstrating asymmetries in non-human animals (Corballis, 2009; Ocklenburg & Gunturkun, 2018; Rogers, Vallortigara, & Andrew, 2013). Nevertheless, fundamental questions that persist are whether there are some asymmetries of the human brain evolved after the separation from the common ancestor with primates and underpinning the human specific adaptation and cognitive ability? The search of such human-specific features is best determined through comparative study with our closest living relative - the chimpanzee (Rilling et al., 2011).

As with many comparative brain studies, identifying species-specific features of lateralization is challenging given the substantial variation in the overall size of the brain and the definition of anatomical regions of interest (ROI) in different species (Keller, Deppe, Herbin, & Gilissen, 2012; Keller et al., 2007). In addition, different computational methods may be adopted for the quantification of brain measures for difference species, which makes the comparison difficult. Based on brain mapping techniques, surface-based morphometry (SBM) analysis enables the projection of brains of difference size to a common standard so that the established inter-subject correspondence allows direct comparison between subjects across the whole cortical surface on a vertex-by-vertex basis. For the examination of inter-hemispheric brain asymmetry, Greve et al. (2013) further proposed an approach to establish the inter-hemispheric correspondence by projecting both cerebral hemispheres to a left-right symmetric registration atlas. The pipeline has been integrated in the FreeSurfer suite and gained popularity in the study of human brain asymmetry. However, relevant application on the chimpanzee brain is very few in the literature. In our previous brain morphology study (Xiang, Crow, & Roberts, 2019a, 2019b; 2018), we adopted Greve's approach to compare the inter-hemispheric positional brain asymmetry between humans and chimpanzees under the same framework. The findings suggested absence of cerebral torque in the chimpanzee brain, contradict to the previous literature (Balzeau & Gilissen, 2010; Hopkins & Marino, 2000; LeMay, 1982). In the present study, we have extended our research and examined the asymmetry of two fundamental measurements which characterize the cerebral cortex, namely surface area (SA) and cortical thickness (CT).

Based on pre-labelled atlases, such as the Desikan-Killiany atlas (Desikan et al., 2006) in the FreeSurfer Image Analysis Suite (http://surfer.nmr.mgh.harvard.edu), brain measures can be summarized in particular ROIs. Specially, there are two parcellation atlases independently constructed for the left and right cerebral hemispheres based on the corresponding manual labelling of a series of brain images. In many studies, these two atlases were employed to separately compute regional value for each cerebral hemisphere and the asymmetry was the difference between values of hemispheres. Given the regional computation procedure relies on two standards, i.e. one atlas for each cerebral hemisphere, we refer this conventional approach as a two-atlas parcellation scheme (TAPS). However, as shown in Figure S1 (a) of the Supplementary Materials, there is significant areal difference between the left and right side of the Desikan-Killiany atlas that reflects the inherent asymmetry of the human brain and as demonstrated in Figure S1 (b) in the Supplementary Materials, different

numbers of vertices are thereby assigned to corresponding ROIs in the left and right cerebral hemispheres of the atlas. More vertices are allocated to the ROI of larger area than to the smaller area. For example, there are 1454 vertices in the larger left PT in comparison to 1022 vertices in the smaller right PT according to Destrieux atlas (Destrieux, Fischl, Dale, & Halgren, 2010). We are concerned that the areal asymmetry in the atlas may be propagated to the regional parcellation for individual subjects and systematically affect the result of brain regional measures through differentially distributed vertices. Indeed, in a TAPS-based meta-analysis based on a "largest ever" population of healthy human subjects, Kong et al. (2018) reported much lower variability of SA asymmetry in comparison to that of CT across many databases. Whilst the authors associated the observation with the computation scheme (i.e. TAPS), we agree and specify that the high consistency of SA measures implies strong influence of bias in the parcellation atlas to brain regional analysis. At the stage, this atlas-bias has not yet been evaluated. A new approach for the ROI-based asymmetry analysis is necessary if ROI analyses are to be considered robust.

Insert Table 1 here

The main objective of the present study is to perform a comparative analysis of SA and CT asymmetry between the human and chimpanzee brain. Firstly, the global inter-hemispheric SA and CT asymmetries were examined and compared between species. Secondly, SA and CT asymmetries were accessed on a vertex-by-vertex basis. Thirdly, a novel approach was developed for the ROI-based asymmetry analysis which we have named single-atlas parcellation scheme (SAPS). Compared to TAPS, SAPS additionally employs the established vertex-wise correspondence between the left and right cerebral hemispheres and therefore is able to project the anatomical convention from a single parcellation atlas (e.g. left or right side of the parcellation atlas) to both the corresponding and the contralateral cerebral hemispheres of individual subjects.

2. Methods

2.1 Subjects and MRI Data Acquisition

MR imaging of humans was conducted at the Queen's Medical Research Institute (QMRI), University of Edinburgh, UK and the Oxford Centre for Magnetic Resonance (OCMR), University of Oxford, UK. Altogether, there are 91 healthy subjects (39 females and 52 males, average age 33.5±12.0 years) in the study, 42 recruited in Edinburgh and 49 recruited in Oxford. Handedness information was recorded for 31 subjects in the Edinburgh group, in which four are left-handed, two have ambiguous handedness and the rest are right-handed, and for 47 subjects in the Oxford group, in which two are left-handed and the rest are right-handed. MR imaging of chimpanzees was conducted at Yerkes National Primate Research Centre (YNPRC) in Atlanta, Georgia, US. There are 77 chimpanzees (50 females and 27 males, average age 26.2±14.0 years). Approval for this study was obtained separately at each site from the local Research Ethics Committee and human subjects provided fully informed written consent prior to taking part.

In Edinburgh the MR images of human subjects were acquired using a 3 T Verio MRI system (Siemens Medical Systems, Erlangen, Germany) and acquisition parameters for the 3D T1-weighted Magnetization-Prepared Rapid-Acquisition Gradient Echo (MPRAGE) sequence are TR = 2300 ms, TE = 2.98 ms, TI = 900 ms, Flip angle = 9°, FOV = 256 mm x 256 mm and the images have isotropic voxel resolution of 1 mm. In Oxford the MR images of human subjects were acquired using a 1.5 T Sonata MRI system (Siemens Healthineers, Erlangen, Germany) and the acquisition parameters for the 3D T1-weighted fast low-angle shot (FLASH) sequence are TR = 5400 ms, TE = 76 ms, Flip angle = 90°, FOV = 256 mm x 160 mm and the images have isotropic voxel resolution of 1mm. In Atlanta the MR images for the chimpanzees were acquired using a Siemens 3 T Trio MRI system (Siemens Healthineers, Erlangen, Germany) and acquisition parameters for the 3D T1-weighted MPRAGE sequence are TR = 2300 ms, TE = 4.4ms, TI = 1100ms, flip angle = 8°, FOV = 200 mm x 200 mm, data matrix size of 320 x 320 and the images have isotropic voxel resolution of 0.6 mm. The chimpanzees were immobilized by ketamine injection (10 mg/kg) and subsequently anesthetized with propofol (40–60 mg/kg/hr) before transportation to the MRI facility where they were scanned supine with a human head-coil and remained anesthetized (total time ~2 hours) for the MR imaging before returning to the home compound.

2.2 Image Analysis

All MR images were pre-processed in FSL (version 5.0.9, http://fsl.fmrib.ox.ac.uk/fsl/fslwiki/) including skull strip, bias field correction and brain normalization using a 7 degrees of freedom (DoF) transformation including 3 translations, 3 rotations and 1 uniform scaling. Specially, the normalization step registered all brain volume images, particularly the chimpanzee brains, to the standard human MNI152 template while preserving the morphology of the brain. Thereby these pre-processed brains were able to be subsequently put through the standard FreeSurfer pipeline (version 6.0, https://surfer.nmr.mgh.harvard.edu/). In FreeSurfer, a volumetric analysis was firstly performed to label the white matter of the brain and split the brain into two cerebral hemispheres. Secondly, a triangular mesh was generated and deformed to tightly cover the white matter component for each cerebral hemisphere with respect to the intensity gradients between the white matter and grey matter and this mesh is the so-called white matter surface. Thirdly, the white matter surface continued to expand along the direction of the intensity gradients between the gray matter and CSF until it coincided with gray matter surface and this surface is also referred to as the so-called pial surface (Dale 1999). For quality control, we visually inspected the reconstructed brain surface for all subjects.

2.3 Vertex-wise Analysis of Brain Asymmetry

For vertex-wise analysis, as described in (Greve et al., 2013; see also Figure 1 (a)), the inter-hemispheric and between-subject correspondences were established through a non-linear registration that adjusts the vertex coordinates of both the left and right cerebral hemispheres of individual subjects to match the folding pattern (i.e. curvature) of a pre-trained left-right symmetric registration atlas (e.g. lh.fsaverage_sym in FreeSurfer which refers to a symmetric atlas constructed based on an initial left hemispheric atlas) in spherical space. In the case of the human brain, the symmetric registration atlas was already available in FreeSurfer (e.g. lh.fsaverage_sym). Whereas the atlas of the chimpanzee brain was specifically constructed for this study based on the procedure described in (Greve et al., 2013). In brief, for 30 brains selected at random from the chimpanzees cohort: (i) both cerebral hemispheres of each subject were co-registered to an initial left-right symmetric atlas (i.e. lh.fsaverage_sym); (ii) a new atlas was generated by averaging the aligned folding patterns of the left and right hemispheres

for all the subjects in the training pool and (iii) the process was iterated three times to produce the final left-right symmetric registration atlas for the chimpanzee brain. Based on the established correspondences, surface-based measures, i.e. SA and CT, that were resampled to the reference atlas space were compared between hemispheres and across subjects. In particular, surface-based spatial smoothing was performed to increase the signal-to-noise ratio. As shown in Figure S4 of the Supplementary Materials, the asymmetry pattern remains the same under different filter sizes and specially, a Gaussian filter with full-width half-maximum (FWHM) of 15 mm was chosen as it corresponds well with the size of brain petalia and gyri which are the features that are the focus of interest in the study.

Insert Figure 1 here

2.4 ROI-based Analysis of Brain Asymmetry

Firstly, the influence of the atlas-bias in the traditional TAPS-based analysis was investigated. We performed an experiment in which the Desikan-Killiany atlas was applied to measure brain asymmetry in a subset of 14 individuals randomly selected from the human cohort. In particular, the TAPS analysis pipeline was applied to the original 3D MR images of the brain and also to the left-right flipped version of the 3D MR images. As demonstrated in Figure S2 (b) of the Supplementary Materials, 23 of 34 (67.7%) ROIs remain to be in the same asymmetry direction even after the image being flipped and these ROIs overlap with the regions showing the largest atlas bias (see Figure S1 (b) of the Supplementary Materials), suggesting that the atlas-bias significantly influences the result of brain asymmetry when TAPS is used. In addition, positive rather than negative correlation was found between the regional SA asymmetries computed for the original scans and their flipped versions [$r=0.79$, $p<0.001$], and both of which are highly positively correlated to the corresponding asymmetry of the Desikan-Killiany atlas (i.e. asymmetry of number of vertices distributed in corresponding ROIs in the left and right cerebral hemisphere [$r>0.70$, $p<0.001$]), which may explain the high consistency of SA asymmetry across databases observed by Kong et al. (2018). We believe that the CT asymmetry is comparatively less severely affected because that the atlas-bias is inherently an areal difference between hemispheres and also, whilst the SA measures are computed as a sum of values at individual vertices within each ROI the CT measures are computed by means of averaging in which the effect bias is eliminated.

In order to address the above atlas-bias in TAPS-based analysis, we developed a new single-atlas parcellation scheme (SAPS), in which only one parcellation standard is employed at one time to subdivide both cerebral hemispheres of individual subjects. As demonstrated in Figure 1 (c), the regional labels of the left side of the Desikan-Killiany atlas were assigned to both the ipsilateral and contralateral cerebral hemispheres of individual subjects based on their inter-hemispheric correspondence as described in Section 2.3. This approach inherently sets a constraint whereby an identical number of vertices is assigned to the corresponding ROI in each cerebral hemisphere. Whilst in TAPS, as shown in Figure 1 (b), the parcellation convention of each cerebral hemisphere in the Desikan-Killiany atlas can only be projected to the corresponding hemisphere of individual subjects based on the between-subject correspondence (see Figure 1 (d)) but no connection between cerebral hemipsheres was built. Although vertex-wise analyis has been shown to be less prone to choice of left or right side of the registration atlas (i.e. lh.fsaverage_sym or rh.fsaverage_sym, Greve et al. 2013), there is still concern on the projection of regional parcellation to contralateral cerebral hemisphere. Therefore, the same analysis pipeline was repeated but now using the right side of the Desikan-Killiany atlas for brain parcellation and the right side of the FreeSurfer atlas (i.e. rh.fsaverage_sym which refers to a symmetric atlas constructed based on an initial right hemisphere atlas) for the inter-hemispheric co-registration in the vertex-wise analysis. The ROI-based values of SA and CT were thereby an average of the values respectively computed based on the left and right atlases. We visually inspected the surface parcellation results for all the human and chimpanzee subjects. Examples for 10 randomly selected chimpanzee subjects are shown in Figure S3 of Supplementary Materials, which demonstrates that the Desikan-Killiany atlas provides reasonable parcellation results for the chimpanzee brain.

Insert Figure 2 here

2.5 Statistical Analysis

In all of the analyses (i.e. global, vertex-wise and ROI), the asymmetry index (AI) was defined as the normalized difference between the left and right cerebral hemisphere according to the formula of AI = 2*(L-R)/(L+R). For the global and ROI-based analyses, two-tailed one sample *t*-tests and multivariate analysis of variance (MANOVA) were respectively performed to test the significance of inter-hemispheric asymmetry of SA and CT for each species and

examine the sex effect on asymmetries using SPSS Statistics for Mac, Version 22.0 (IBM Corp., Armonk, N.Y., USA). For the vertex-wise analysis, GLM in FreeSurfer was performed at each cortical location on the cerebral surface to identify the clusters of significant SA and CT asymmetries respectively for the human and chimpanzee brains and the regions showing significant between-species difference, followed by a cluster-wise multiple comparison with both the cluster forming and cluster-wise significant levels being set to 0.01. In addition, the Spearman's correlation analysis was performed to explore the consistency of directional asymmetry between the human and chimpanzee brain based on the ranked order of the asymmetry indices across 34 ROIs of the Desikan-Killiany atlas.

3. Results

3.1 Global SA and CT asymmetry

The mean values of SA and CT in the left and right cerebral hemispheres are presented in Table 2 for the human and chimpanzee brain. For the human brain, total SA is significantly larger in the right compared to the left cerebral hemisphere [$t(90) = -4.10$, $p < 0.001$] but there is no significant population-level asymmetry for CT. For the chimpanzee brain, no significant population-level asymmetry was found for either SA or CT. MANOVA showed no main effect of sex on SA or CT asymmetry in either the human [$F(2,88) = 1.23$, $p = 0.30$] or chimpanzee [$F(2,74) = 0.67$, $p = 0.52$] brain.

3.2 Vertex-wise and ROI-based SA Asymmetry

According to Figure 2 (a), the vertex-wise analysis for the human brain revealed significant rightward SA asymmetry in the (i) STS extending to posterior insula, (ii) inferior parietal and (iii) medial frontal and (iv) medial occipital cortex. In contrast, significant leftward asymmetry was found in the (v) supra-marginal gyrus extending to PT and (vi) anterior insula extending to Broca's area and anterior and inferior temporal lobe. In comparison, the vertex-wise analysis for the chimpanzee brain showed significant leftward asymmetry in the (i) Sylvian fissure extending from anterior superior temporal to supra-marginal gyrus and (ii) inferior parietal cortex and cuneus, but there are no significant population-level rightward asymmetries. The comparative analysis further revealed significant species difference in the (i) STS, (ii) posterior insula, (iii) inferior parietal, (iv) inferior temporal, (v) medial frontal and (vi) medial occipital and (vii) supra-marginal gyrus. According to the average SA asymmetry map computed for individual species in Figure 4 (a), only the species difference in the supra-marginal gyrus is due to a magnitude difference while in the remaining regions, SA asymmetries are in opposite directions between the human and chimpanzee brain.

The result of the ROI-based analysis of SA asymmetry is depicted in Figure 3 (a). There are a greater number of ROIs showing significant asymmetry in the human brain (i.e. in 10 of 34 ROIs) compared to the chimpanzee brain (i.e. in 2 of 34 ROIs). The statistics of regional SA asymmetries are summarized in Table 3 and the measurements of SA for the 34 ROIs per cerebral hemisphere of the Desikan-Killiany atlas are provided in Table S1 of the Supplementary Materials respectively for the human and chimpanzee brain.

MANOVA revealed no significant main effect of sex on the overall SA asymmetry in either the human [$F(34,56) = 1.51$, $p = 0.08$] or chimpanzee [$F(34,42) = 0.92$, $p = 0.60$] brain. Although, subsequent univariate ANOVA showed significant effect of sex on SA asymmetry

in the superior temporal lobe [$F(1,89) = 9.56$, $p = 0.003$], cuneus [$F(1,89) = 5.61$, $p = 0.02$], pars opercularis [$F(1,89) = 4.75$, $p = 0.03$] and pars triangularis [$F(1,89) = 8.19$, $p = 0.01$] for the human brain and in bankssts [$F(1,75) = 5.39$, $p = 0.02$] and inferior parietal [$F(1,75) = 4.11$, $p = 0.05$] for the chimpanzee brain, however, none survived Bonferroni correction for multiple comparisons.

3.3 Vertex-wise and ROI-based CT Asymmetry

According to Figure 2 (b), the vertex-wise analysis of CT asymmetry for the human brain revealed significant rightward asymmetry in the (i) temporal and (ii) occipital lobes and significant leftward asymmetry in the (iii) superior and middle frontal gyrus. In comparison, the vertex-wise analysis for the chimpanzee brain revealed significant rightward asymmetry in the (i) pre-central gyrus, (ii) paracentral gyrus and significant leftward asymmetry in the (iii) dorsal anterior cingulate. The comparative analysis further revealed significant species differences in the (i) STS, (ii) medial occipital and (iii) pre-central cortex. According to the average asymmetry map computed for individual species shown in Figure 4 (b), in all these areas exhibiting significant species difference, CT asymmetries are in opposite directions between the human and chimpanzee brain.

The results of the ROI-based analysis of CT asymmetry is depicted in Figure 3 (b). There are 9 out of 34 ROIs showing significant population-level asymmetry in the human brain compared to 7 out of 34 ROIs in the chimpanzee brain. The statistics of regional CT asymmetry are shown in Table 4 and the measurements of CT for the 34 ROIs per cerebral hemisphere of the Desikan-Killiany atlas are summarized in Table S2 of the Supplementary Materials for the human and chimpanzee brain. Most notably, both the vertex-wise and ROI-based analysis showed that the frontal lobe is thicker in the left compared to the right cerebral hemisphere and the temporo-parieto-occipital lobe is thicker in the right compared to the left cerebral hemisphere in the human brain, a pattern that is not present in the chimpanzee brain.

MANOVA revealed no significant main effect of sex on CT asymmetry in either the human [$F(34,56) = 0.79$, $p=0.76$] or chimpanzee [$F(34,42) = 0.54$, $p = 0.97$] brain, neither did subsequent ANOVA in any ROIs.

Insert Figure 2 here

Insert Figure 3 here

Insert Figure 4 here

3.4 Relationship between Asymmetries in the Human and Chimpanzee Brain

We are also interested in whether variation in the direction and magnitude of asymmetries in SA and CT are similar or different between the human and chimpanzee brain. The correlation analysis revealed that for CT, but not SA, there is modest and marginally significant consistency in the strength and direction of asymmetries across 34 ROIs between humans and chimpanzees [CT: $r = 0.34$, $p = 0.05$; SA: $r = 0.15$, $p = 0.40$]. Whereas the correlation analysis between SA and CT asymmetry showed that on average there is no significant relationship between SA and CT asymmetry in either the human [$r = 0.08$, $p = 0.64$] or the chimpanzee [$r = 0.31$, $p = 0.08$] brain.

4. Discussion

We performed a comparative study of SA and CT asymmetries in the human and chimpanzee brain. Overall, the results revealed that asymmetries are more extensive in the former than the latter given that globally, there is significantly greater SA in the right compared to the left cerebral hemisphere in and only in the human brain, and locally, population-level SA asymmetry was observed in 10 of 34 (29.4%) ROIs and CT asymmetry in 9 of 34 (26.5%) ROIs for the human brain, compared with respective values of 2 of 34 (5.9%), and 7 of 34 (20.6%) ROIs for the chimpanzee brain. In addition, there is significant difference between the human and chimpanzee brain and it largely arises from the difference in the pattern of asymmetry rather than the difference in the magnitude of asymmetry between species. In particular, human-specific population-level SA asymmetries were found in the STS, insula, supra-marginal gyrus, inferior parietal, medial occipital, medial orbital frontal and anterior cingulate and CT asymmetries in the middle temporal and medial occipital gyrus, whereas chimpanzee-specific population-level asymmetry was observed only in the pre-central gyrus for CT.

In the present study we addressed the atlas-bias in the conventional ROI-based analysis. Specially, a novel parcellation scheme called SAPS was developed for the regional analysis. The development of the SAPS approach as compared to the TAPS approach is broadly equivalent to the use of a symmetric compared to a standard atlas in Voxel Based Morphometry (VBM) studies. In particular, when an atlas is developed by using the image registration technique to combine the images of individuals in a cohort, if there is an average asymmetry in the population this will appear in the atlas (see Figure S1 of the Supplementary Materials). If the atlas is then used in a new study this asymmetry can potentially add asymmetry to a population of individuals in which no asymmetry is present. Since our previous studies have shown that the chimpanzee brain is more symmetrical than the human brain (e.g. Xiang et al., 2018) we had concerns that by using TAPS the inherent asymmetry of the human Desikan-Killiany atlas could be propagated to the chimpanzee brain. In SAPS, because an equivalent number of vertices is assigned to refer to each ROI in the left cerebral hemisphere and the corresponding ROI in the right cerebral hemisphere, it limits the propagation of asymmetry that may arise from there being different numbers of vertices associated with the corresponding ROI's in the left or right cerebral hemisphere (see Figure S1 (b) of the Supplementary Materials). In addition, the averaging which occurs as the last step in the SAPS analysis resembles the construction of a symmetric atlas in the VBM approach (i.e. an averaging between the standard atlas and its mirror reflection). For each ROI, measurements derived from

the left and right sides of the parcellation atlas are averaged to avoid the possibility of bias if only one side had been used. Demonstration that SAPS provides a less biased approach for the ROI-based analysis of cerebral asymmetry is provided in Figure S2 of the Supplementary Materials. In brief, the analysis pipeline of SAPS was applied to the original 3D MR images of 14 brains and also to left-right flipped versions of the same images. In Figure S2 it can be clearly seen that the results are almost completely reversed in the case when SAPS is used but not when TAPS is used. This observation is supported quantitatively in that the SA asymmetry measurements remained in the same direction in 23 of 34 ROIs (i.e. 67.7%) when TAPS was used but only in 4 of 34 ROIs (11.8%) when SAPS was applied. In addition, whilst the regional SA asymmetries computed using TAPS are highly determined by the asymmetry in the Desikan-Killiany atlas ($r > 0.7$, $p < 0.005$), i.e., asymmetry of number of vertices distributed in corresponding ROIs in the left and right cerebral hemisphere, this is not the case when using SAPS, which further demonstrates that the latter is less prone to the atlas-bias.

Regarding the SA asymmetry in the human brain, in agreement with the meta-analysis performed by Kong et al. (2018), we found that the total brain SA is significantly larger on the right cerebral hemisphere compared to the left, and there is leftward asymmetry in the transverse temporal gyrus, superior temporal, inferior temporal, supra-marginal gyrus and rightward asymmetry in the middle temporal cortex, inferior parietal, cuneus and peri-calcarine. However, we failed to reproduce the rightward asymmetry in the anterior and leftward asymmetry in the posterior Broca's area, where show the largest atlas-bias (see Figure S1 of the Supplementary Materials). In addition, the finding of significant leftward asymmetry of a region in the anterior Broca's area extending to the lateral orbital frontal and anterior temporal cortex is consistent with the observation in another vertex-wise analysis by Lyttelton et al. (2009), and significant leftward asymmetry of the parahippocampal gyrus and significant rightward asymmetry of the medial orbital frontal are consistent with the findings by Van Essen et al. (2012). In the case of CT asymmetry, a marked pattern was found in the human brain, corresponding to the relatively thicker gray matter cortex in the left compared to the right frontal lobe and the right compared to the left temporo-parieto-occipital lobe which forms the pattern of torque. This finding is consistent with the observations by Plessen et al. (2014), Luders et al. (2006) and Le Guen et al. (2018b), however, opposite to the findings of Zhou et al. (2013) and Maingault et al. (2016). Lateralization has also been reported for the white matter underlaying the gray matter. For example, the white matter (i.e. arcuate fasciculus) which links lateral temporal cortex and frontal lobe has been reported to be both structurally and functionally asymmetric (Takaya et al., 2015; Trivedi et al., 2009). Furthermore, Rilling et al.

(2011) reported that there has been a remarkable augmentation of this dorsal language pathway in human evolution, and which is more pronounced in the left hemisphere and is suggested to be related to the development of language. The potential relationship between the asymmetry of the gray matter and white matter is an important topic for further investigation.

Two brain areas were found to be asymmetric in both the SA and CT analyses in the human brain. They are the medial occipital lobe and STS. Both showed reduction of SA and CT on the left compared to the right. In the case of the medial occipital lobe, the observation is compatible with the greater posterior extension and rightward bending that were previously reported in the occipital lobe (Xiang et al., 2018) and rightward gyrification asymmetry in the associated region was also reported by Chiarello et al. (2016). In the case of STS, the finding supports the superior temporal asymmetrical pit (STAP) asymmetry identified by Leroy et al. (2015) as the "new human specific landmark", which has been later found to be genetically constrained (Le Guen et al., 2018a; Le Guen et al., 2018b), advocating its potential role for the language specification developed during very recent evolution. Of further interest with respect of the human brain is the finding of opposite directions of SA asymmetry in the anterior (i.e. leftward) and posterior insula (i.e. rightward). This finding may help to resolve the discrepancy between asymmetries previously reported for this brain region. In particular, Watkins et al. (2001) performed a VBM-based asymmetry study in 142 healthy subjects and reported significant rightward asymmetry whereas Keller et al. (2011) performed a stereological analysis to measure insula volume in 25 subjects with confirmed hemisphere language dominance (HLD) and reported leftward insula asymmetry to be associated with left HLD. The respective blue and red coloured regions overlying the anterior and posterior insula in the second panel of the top row of Figure 2 and which are compatible with the respective findings of Watkins et al. (2001) and Keller et al. (2011), respectively, and not present in the results of the ROI-based analysis of the first panel of the same row, indicate that the averaging inherent in the use of predefined ROI's may obscure findings of interest.

The chimpanzee brain shows less areas of significant population-level SA and CT asymmetry than the human brain and no significant population-level asymmetry in the global SA and CT. In contrast to previous post-mortem studies by Hopkins and Avants (2013), and Cantalupo and Hopkins (2001), we did not find extensive CT asymmetry in frontal, parietal and temporal lobes, except for the rightward asymmetry in the pre-central gyrus, and significant leftward SA asymmetry of the Broca area, respectively. The observation of significant rightward CT asymmetry in the pre-central gyrus specific to the chimpanzee brain is a new finding. Larger proportionally compared to Old World monkeys, the primary motor

region of the chimpanzee brain has the thinnest cortex across the whole cerebral surface (Hopkins & Avants, 2013; Hopkins et al., 2016). After taking account of brain size, it is also disproportionately thinner than in humans (Hopkins et al., 2016). At the cellular level, a post-mortem study of 18 chimpanzees revealed that the density asymmetry of parvalbumin-immunoreactive interneurons in layers II and III of primary motor cortex to be significantly related to hand preference (Sherwood, Wahl, Erwin, Hof, & Hopkins, 2007). These evidences suggest that structural asymmetry of primary motor cortex may be related to the evolution of handedness (Hopkins & Cantalupo, 2004). Nevertheless, cautions still need be taken in interpreting the functional significance of this asymmetric feature. Because on the one hand the present study showed humans who have more definite handedness preference do not present any asymmetry in this region. On the other hand, large sample size studies of humans have also failed to find significant association between asymmetry of primary motor cortex and handedness (Good et al., 2001; Kong et al., 2018; Wiberg et al., 2019), nor any cortical structural correlates of handedness (Guadalupe et al., 2014).

The present study provides substantial evidence on that humans and chimpanzees show different patterns of asymmetry. Specially, the direction of asymmetry in the region showing significant species difference is on average opposite between the human and chimpanzee brain (see Figure 4). In addition, the species difference in most cases arises from distinctive asymmetry in the human brain which is absent in the chimpanzee brain on a population-level, with one exception in the pre-central cortex. In this context, the divergence of asymmetry found here challenges the view of gradual process of evolution in which chimpanzees are considered to share the same pattern of asymmetry as humans but only differ in a matter of magnitude (Gomez-Robles, Hopkins, & Sherwood, 2013). The presence of asymmetries in the chimpanzee brain, though few in number, also provides further confirmation that population-level asymmetry is not unique to Homo sapiens. Population-level behavioural, functional and anatomical asymmetries have been previously reported in a wide range of primates (Corballis, 2009; Holloway & De La Costelareymondie, 1982; Hopkins, Misiura, Pope, & Latash, 2015). Holloway and De La Coste-Lareymondie (1982) were the first to study brain asymmetry in pongids (i.e. great apes) and hominids (i.e. humans and their fossil ancestors). They reported that while all taxa of hominoids (i.e. both groups) show asymmetries to various degrees, the patterns or combination of petalial asymmetries are very different. Only modern Homo and hominids (Australopithecus, Homo erectus, Neandertals) show a distinct left-occipital, right-frontal petalial asymmetry pattern. Of the pongids, gorilla shows leftward asymmetry of the occipital petalias. Subsequently, in a study of formalin fixed brain specimens of 5 Old and New

World Monkey species, Heilbroner and Holloway (1988) reported significantly greater Sylvian fissure length in the left compared to the right cerebral hemisphere, as is typical in humans (Hou et al., 2019), in four of the species. Corresponding population-level leftward asymmetries of PT have also been reported for chimpanzees (Gannon, Holloway, Broadfield, & Braun, 1998; Hopkins & Nir, 2010; Zilles et al., 1996) and baboons (Marie et al., 2017) but not in macaque monkeys (Gannon, Kheck, & Hof, 2008; Lyn et al., 2011). Hopkins et al., (2015) have investigated whether hemispheric specialization evolved as a by-product of increasing brain size relative to the surface area of the corpus callosum. They report that species with larger brains have relatively small corpus callosi, suggesting that humans have increasingly "split" or "disconnected" hemispheres, followed by great apes, then Old World monkeys. Nevertheless, as the present and previous studies have shown (Xiang et al., 2018; Xiang et al., 2019a and b) certain population level asymmetries are, however, unique to the human brain (Crow, 2004; Crow, 2010). We believe that the common ancestor of humans and great apes had already present cortical asymmetry, most likely in the peri-Sylvian region, such as leftward SA asymmetry in PT. After the separation from the common ancestor, brain asymmetry appears to have developed independently in individual species, influenced by both genetic and environmental factors. The new and more extensive asymmetries of the medial occipital lobe and STS in the human brain are more likely to be related to the lateralization in cognitive abilities, such as left hemisphere dominance for language.

The failure to detect a significant correlation between SA and CT asymmetry in either species is consistent with the previous studies in humans (Winkler et al. 2010) and chimpanzees (Hopkins & Avants, 2013), supporting that SA and CT have developmental phenotypes that are presumably dependent upon different factors (Panizzon et al., 2009; Winkler et al., 2010). Albeit, interestingly, a marginally significant correlation was observed between asymmetries of the human and chimpanzee brain in CT ($p = 0.05$), but not SA. This finding suggests that the human brain can be better distinguished from the chimpanzee brain on the basis of SA rather than CT asymmetry, which is in line with the claim that more substantial change existing in SA than CT during the course of human evolution (Lyall et al., 2015; Meyer, Liem, Hirsiger, Jancke, & Hanggi, 2014; Rakic, 1995), and it is also relevant to another observation that general cognitive ability is driven by SA rather than CT (Vuoksimaa et al. 2015). In this context, our result points out that the search for neural structural basis underlying superior human cognitive ability in comparative studies should be more fruitful if it is based on SA.

There is no significant sex effect on brain SA or CT at the global level for either species. However, an interesting sexual dimorphism of SA asymmetry is observed in the superior temporal lobe in the human brain. In particular, males were found to be significantly more leftward asymmetric in this brain region than females ($p<0.001$). The sex difference was significant ($p=0.003$), though did not survive Bonferroni correction for multiple comparisons. Kong et al. (2018), also reported a sex difference in the same region in investigating a larger cohort of healthy subjects. In an aneuploidy study, based on the observation of more pronounced asymmetry in XY males than XX females and XXY males within the superior temporal lobe, Savic (2014) raised the possibility that the associated region to be responsible for the sex difference that has been widely reported in speech processing.

A limitation of the study is that the gyral boundaries used for parcellation of the chimpanzee brain are derived from the Desikan-Killiany neuro-anatomical atlas of the human brain (Desikan et al., 2006) which was constructed by averaging boundaries manually delineated for 34 ROIs on the basis of relevant gyri in each cerebral hemisphere of co-registered 3D MRI scans obtained for 40 individuals. In several previous studies the brains of individual subjects in human and chimpanzee cohorts have been co-registered to a common reference space using the FreeSurfer pipeline (Xiang et al., 2018; Xiang et al., 2019a and b) and in one study the Desikan-Killiany atlas was applied to compare corresponding ROIs in the human and chimpanzee brain (Hopkins et al., 2017). In each case the co-registration using FreeSurfer is checked by using rigorous quality control procedures (Xiang et al. 2018) and the subsequent use of the Desikan-Killiany atlas is possible because the average pattern of the primary, and many of the secondary and tertiary gyri, is closely similar in the human and chimpanzee brain. Thus although within the 34 ROIs in each cerebral hemisphere there are undoubtedly variations in the gyral pattern, as shown in Figure S3 of Supplementary Materials the bounding gyri show close correspondence between the human and chimpanzee brain. Besides, the SAPS-based regional result is highly consistent with the vertex-wise result that is less prone to the above mentioned atlas-bias. In an alternative approach to atlas-based ROI analysis, Le Guen et al. (2018a; 2018b) proposed a novel strategy. In particular, the location of sulcal pits in the left and right cerebral hemispheres of individual subjects is determined and then a watershed algorithm is applied to define mutual boundaries for new ROIs in each cerebral hemispheres. The method essentially generates a study-specific symmetric parcellation standard for subsequent regional analysis and is likely to be widely employed in future studies. The approach is not, however, as suitable for use in the present comparative study as it is unlikely that the two species share the same pattern of distribution of sulcal pits. Another limitation is

the lack of investigation of handedness effect on brain asymmetries, which was infeasible because of the incompleteness of handedness information for the human cohort. Although, as mentioned before, no significant association between brain asymmetries and handedness was detected for any of the ROI's in the meta-analysis performed by Kong et al. (2018) (see also the vertex-wise SA and CT asymmetry analysis reported by Maingault et al. (2016)). It should also be emphasised that inconsistencies with results reported in other studies could be related to (i) methodological differences such as use of SAPS compared to TAPS, use of SBM rather than VBM and use of automatic compared to manual methods (e.g. automatic parcellation versus manual outlining of ROIs), (ii) spatial resolution (e.g. 163,842 vertices per cerebral hemisphere in the present study compared to 40,962 vertices per cerebral hemisphere in the study by (Zhou et al., 2013)), (iii) statistical methods, (iv) *in*-vivo versus *in*-vitro studies and (v) sample size considerations.

In summary, we have presented the most comprehensive comparison so far available for SA and CT asymmetry between the human and chimpanzee brain. Overall, the human brain shows much greater asymmetry with distinct global and local features, whereas the chimpanzee brain is comparatively less asymmetric with seemingly only local asymmetries being present rather than having a global pattern of asymmetry such as the torque. The species difference is qualitative rather than quantitative. In most regions where present significant difference between the human and chimpanzee brain, the sign of the average brain asymmetry is in opposite direction. Thus, it is probably not true that the two species share the same asymmetry but which is only more prominent in humans (Gomez-Robles et al., 2013).

With regard to local asymmetries that are present in the human and chimpanzee brain, there is diminishing evidence for the one that was long predicted and expected to be found in Broca's area and its homologue, but on the other hand increasing evidence that both species share a common leftward asymmetry in PT and its homologue. Accordingly, against the backdrop of a global torque present in only the human brain is the interesting finding that the two species likely share an identical pattern of presence, and absence, of structural asymmetries in receptive, and expressive, "language" areas. Added to this are intriguing findings of structural asymmetries unique to each species, namely we found further support for the rightward STS asymmetry proposed by Leroy et al. (2015) to be a human-specific landmark and observed for the first time a chimpanzee-specific asymmetry of the precentral gyrus and which could possibly provide information relevant to deciphering the brain changes that may have occurred related to the evolution of handedness.

In conclusion, after being highly sought after for well over a century but remaining somewhat enigmatic, a clearer picture is finally emerging regarding the nature of structural brain asymmetry and its evolution and many interesting lines of enquiry can now be more confidently pursued. The above mentioned asymmetries are all relatively subtle, but they are real, and they may be measured in unprecedented detail by using state of the art MR imaging and image analysis techniques such as those used in the present study and which are becoming ever more refined and sophisticated. Coupled with advances in genetics, "Big Data" and artificial intelligence we anticipate the study of structural brain asymmetries is poised to lead to new knowledge and new understanding regarding brain evolution and brain structural and functional organisation and we hope that the findings of the present study will provide further motivation to conduct these analyses.

Acknowledgments

LX was supported by T.J. Crow Psychosis Research Trust and WDH was supported by NIH grant NS-42867 and HD-60563. We thank Prof. Stephen Lawrie for access to MRI scans of human subjects at the University of Edinburgh and staff at the University of Edinburgh, University of Oxford and Yerkes National Primate Center for their support in acquiring the MRI data.

References

Amunts K, Schlaug G, Schleicher A, Steinmetz H, Dabringhaus A, Roland PE, Zilles K. 1996. Asymmetry in the human motor cortex and handedness. Neuroimage. 4(3 Pt 1):216-222.

Balzeau A, Gilissen E. 2010. Endocranial shape asymmetries in *pan* paniscus, *pan* troglodytes and gorilla gorilla assessed via skull based landmark analysis. J Hum Evol. 59:54-69.

Balzeau A, Gilissen E, Grimaud-Herve D. 2012. Shared pattern of endocranial shape asymmetries among great apes, anatomically modern humans, and fossil hominins. PLoS One. 7(1):e29581.

Cantalupo C, Hopkins WD. 2001. Asymmetric Broca's area in great apes. Nature. 414(6863):505.

Chiarello C, Vazquez D, Felton A, McDowell A. 2016. Structural asymmetry of the human cerebral cortex: Regional and between-subject variability of surface area, cortical thickness, and local gyrification. Neuropsychologia. 93(Pt B):365-379.

Corballis M. 2004. Laterality and human speciation. Proceedings of the British Academy. p: 136-152.

Crow T. 2004. Directional asymmetry is the key to the origin of modern *homo* sapiens (the Broca-Annett axiom): A reply to Rogers' review of the speciation of modern *homo* sapiens. Laterality: Asymmetries of Body, Brain and Cognition. 9:233-242.

Crow TJ. 2010. A theory of the origin of cerebral asymmetry: Epigenetic variation superimposed on a fixed right-shift. Laterality. 15:289-303.

Cunningham DJ. 1892. Contribution to the surface anatomy of the cerebral hemispheres. Cunningham Mem (R Ir Acad). 7(372).

Dale AM, Fischl, B., Sereno, M.I. 1999. Cortical surface-based analysis I: Segmentation and surface reconstruction. NeuroImage. 9:179-194.

Desikan RS, Segonne F, Fischl B, Quinn BT, Dickerson BC, Blacker D, Buckner RL, Dale AM, Maguire RP, Hyman BT et al. 2006. An automated labeling system for subdividing the human cerebral cortex on MRI scans into gyral based regions of interest. Neuroimage. 31:968-980.

Destrieux C, Fischl B, Dale A, Halgren E. 2010. Automatic parcellation of human cortical gyri and sulci using standard anatomical nomenclature. Neuroimage. 53:1-15.

Eberstaller O. 1884. Zür oberflachen anatomie der grosshirn hemisphaeren. Wien Med. 7(479):642-644.

Eberstaller O. 1890. Das stirnhirn. Ein beitrag zur anatomie der oberfläche des grosshirns. Urban and schwarzenberg, wien und leipzig.

Foundas AL, Eure KF, Luevano LF, Weinberger DR. 1998. MRI asymmetries of Broca's area: The pars triangularis and pars opercularis. Brain Lang. 64(3):282-296.

Gannon PJ, Holloway RL, Broadfield DC, Braun AR. 1998. Asymmetry of chimpanzee planum temporale: Humanlike pattern of Wernicke's brain language area homolog. Science. 279(5348):220-222.

Geschwind N, Levitsky W. 1968. Human brain: Left-right asymmetries in temporal speech region. Science. 161(3837):186-187.

Gomez-Robles A, Hopkins WD, Sherwood CC. 2013. Increased morphological asymmetry, evolvability and plasticity in human brain evolution. Proc Biol Sci. 280(1761):20130575.

Good CD, Johnsrude I, Ashburner J, Henson RN, Friston KJ, Frackowiak RS. 2001. Cerebral asymmetry and the effects of sex and handedness on brain structure: A voxel-based morphometric analysis of 465 normal adult human brains. Neuroimage. 14(3):685-700.

Greve DN, Van der Haegen L, Cai Q, Stufflebeam S, Sabuncu MR, Fischl B, Brysbaert M. 2013. A surface-based analysis of language lateralization and cortical asymmetry. J Cogn Neurosci. 25(9):1477-1492.

Hopkins WD. 1995. Hand preferences for a coordinated bimanual task in 110 chimpanzees (*pan* troglodytes): Cross-sectional analysis. J Comp Psychol. 109(3):291-297.

Hopkins WD. 2013. Neuroanatomical asymmetries and handedness in chimpanzees (*pan* troglodytes): A case for continuity in the evolution of hemispheric specialization. Ann N Y Acad Sci. 1288:17-35.

Hopkins WD, Avants BB. 2013. Regional and hemispheric variation in cortical thickness in chimpanzees (*pan* troglodytes). J Neurosci. 33(12):5241-5248.

Hopkins WD, Cantalupo C. 2004. Handedness in chimpanzees (*pan* troglodytes) is associated with asymmetries of the primary motor cortex but not with homologous language areas. Behav Neurosci. 118(6):1176-1183.

Hopkins WD, Li X, Crow T, Roberts N. 2016. Vertex- and atlas-based comparisons in measures of cortical thickness, gyrification and white matter volume between humans and chimpanzees. Brain Struct Funct. 222(1):229-245.

Hopkins WD, Meguerditchian A, Coulon O, Bogart S, Mangin JF, Sherwood CC, Grabowski MW, Bennett AJ, Pierre PJ, Fears S et al. 2014. Evolution of the central sulcus morphology in primates. Brain Behav Evol. 84(1):19-30.

Hopkins WD, Nir TM. 2010. Planum temporale surface area and grey matter asymmetries in chimpanzees (*pan* troglodytes): The effect of handedness and comparison with findings in humans. Behav Brain Res. 208(2):436-443.

Hopkins WD, Taglialatela JP, Meguerditchian A, Nir T, Schenker NM, Sherwood CC. 2008. Grey matter asymmetries in chimpanzees as revealed by voxel-based morphometry. Neuroimage. 42(2):491-497.

Hou L, Xiang L, Crow T, Leroy F, Riviere D, Mangin JF, Roberts N. 2018. Measurement of Sylvian Fissure asymmetry and occipital bending in humans and *pan* troglodytes. Neuroimage. 184:855-870.

Keller SS, Crow T, Foundas A, Amunts K, Roberts N. 2009a. Broca's area: Nomenclature, anatomy, typology and asymmetry. Brain Lang. 109(1):29-48.

Keller SS, Deppe M, Herbin M, Gilissen E. 2012. Variability and asymmetry of the sulcal contours defining Broca's area homologue in the chimpanzee brain. J Comp Neurol. 520(6):1165-1180.

Keller SS, Roberts N, Hopkins W. 2009b. A comparative magnetic resonance imaging study of the anatomy, variability, and asymmetry of Broca's area in the human and chimpanzee brain. J Neurosci. 29(46):14607-14616.

Koelkebeck K, Miyata J, Kubota M, Kohl W, Son S, Fukuyama H, Sawamoto N, Takahashi H, Murai T. 2014. The contribution of cortical thickness and surface area to grey matter asymmetries in the healthy human brain. Hum Brain Mapp. 35(12):6011-6022.

Kong XZ, Mathias SR, Guadalupe T, Glahn DC, Franke B, Crivello F, Tzourio-Mazoyer N, Fisher SE, Thompson PM, Francks C. 2018. Mapping cortical brain asymmetry in 17,141 healthy individuals worldwide via the enigma consortium. Proc Natl Acad Sci U S A. 115(22):E5154-e5163.

LeMay M. 1976. Morphological cerebral asymmetries of modern man, fossil man, and nonhuman primate. Ann N Y Acad Sci. 280:349-366.

LeMay M, Billig MS, Geschwind N. 1982. Asymmetries of the brains and skulls of nonhuman primates. In: E. Armstrong DF, editor. Primate brain evolution methods and concepts. New York: Plenum Press. p:263–277.

Leroy F, Cai Q, Bogart SL, Dubois J, Coulon O, Monzalvo K, Fischer C, Glasel H, Van der Haegen L, Benezit A et al. 2015. New human-specific brain landmark: The depth asymmetry of superior temporal sulcus. Proc Natl Acad Sci U S A. 112(4):1208-1213.

Luders E, Narr KL, Thompson PM, Rex DE, Jancke L, Toga AW. 2006. Hemispheric asymmetries in cortical thickness. Cereb Cortex. 16(8):1232-1238.

Lyall AE, Shi F, Geng X, Woolson S, Li G, Wang L, Hamer RM, Shen D, Gilmore JH. 2015. Dynamic development of regional cortical thickness and surface area in early childhood. Cereb Cortex. 25(8):2204-2212.

Lyn H, Pierre P, Bennett AJ, Fears S, Woods R, Hopkins WD. 2011. Planum temporale grey matter asymmetries in chimpanzees (*pan* troglodytes), vervet (chlorocebus aethiops sabaeus), rhesus (macaca mulatta) and bonnet (macaca radiata) monkeys. Neuropsychologia. 49(7):2004-2012.

Lyttelton OC, Karama S, Ad-Dab'bagh Y, Zatorre RJ, Carbonell F, Worsley K, Evans AC. 2009. Positional and surface area asymmetry of the human cerebral cortex. Neuroimage. 46(4):895-903.

Maingault S, Tzourio-Mazoyer N, Mazoyer B, Crivello F. 2016. Regional correlations between cortical thickness and surface area asymmetries: A surface-based morphometry study of 250 adults. Neuropsychologia. 93(Pt B):350-364.

Meyer M, Liem F, Hirsiger S, Jancke L, Hanggi J. 2014. Cortical surface area and cortical thickness demonstrate differential structural asymmetry in auditory-related areas of the human cortex. Cereb Cortex. 24(10):2541-2552.

Balzeau, A., & Gilissen, E. (2010). Endocranial shape asymmetries in *Pan* panuscus*, Pan* troglodytes, and *Gorilla* gorilla assessed via skull based landmark analysis. Journal of Human Evolution, 59, 54-69.

Barrick, T. R., Lawes, N., Mackay, C. E., & Clark, C. A. (2007). White matter pathway asymmetry underlies functional lateralization. Cerebral Cortex, 17(3), 591-598.

Bradshaw, B., & Rogers, L. (1993). The evolution of lateral asymmetries, language, tool-use and intellect. San Diego: Academic Press.

Cantalupo, C., & Hopkins, W. D. (2001). Asymmetric Broca's area in great apes. Nature, 414(6863), 505. doi:10.1038/35107134

Chiarello, C., Vazquez, D., Felton, A., & McDowell, A. (2016). Structural asymmetry of the human cerebral cortex: Regional and between-subject variability of surface area, cortical thickness, and local gyrification. Neuropsychologia, 93(Pt B), 365-379. doi:10.1016/j.neuropsychologia.2016.01.012

Corballis, M. C. (1992). The lopsided brain: Evolution of the generative mind. New York: Oxford University Press.

Corballis, M. C. (2002). From hand to mouth:The origins of language. Princeton, NJ: Princeton University Press.

Corballis, M. C. (2009). The evolution and genetics of cerebral asymmetry. Philos Trans R Soc Lond B Biol Sci, 364(1519), 867-879. doi:10.1098/rstb.2008.0232

Crow, T. J. (2009). A theory of the origin of cerebral asymmetry: Epigenetic variation superimposed on a fixed right-shift. Laterality, 15(3), 289-303.

Cunningham, D. J. (1892). Contribution to the surface anatomy of the cerebral hemispheres. Cunningham Mem. (R. Ir. Acad.), 7(372).

Dale, A. M., Fischl, B., Sereno, M.I. (1999). Cortical Surface-Based Analysis I: Segmentation and Surface Reconstruction. NeuroImage, 9(2), 179-194

Desikan, R. S., Segonne, F., Fischl, B., Quinn, B. T., Dickerson, B. C., Blacker, D., Killiany, R. J. (2006). An automated labeling system for subdividing the human cerebral cortex on MRI scans into gyral based regions of interest. Neuroimage, 31(3), 968-980. doi:10.1016/j.neuroimage.2006.01.021

Eberstaller, O. (1884). Zür Oberflachen Anatomie der Grosshirn Hemisphaeren Wien Med, 7(479), 642-644.

Eberstaller, O. (1890). Das Stirnhirn. Ein Beitrag zur Anatomie der Oberfläche des Grosshirns. Urban & Schwarzenberg, Wien und Leipzig.

Fischl, B., Sereno, M. I., Tootell, R. B., & Dale, A. M. (1999). High-resolution intersubject averaging and a coordinate system for the cortical surface. Hum Brain Mapp, 8(4), 272-284. doi:10.1002/(sici)1097-0193(1999)8:4<272::aid-hbm10>3.0.co;2-4

Gannon, P. J., Holloway, R. L., Broadfield, D. C., & Braun, A. R. (1998). Asymmetry of chimpanzee Planum Temporale:Humanlike pattern of Wernicke's language area homolog. Science, 279, 220-222.

Gannon, P. J., Kheck, N., & Hof, P. R. (2008). Leftward interhemispheric asymmetry of macaque monkey temporal lobe language area homolog is evident at the cytoarchitectural, but not gross anatomic level. Brain Research, 1199, 62-73.

Geschwind, N., & Levitsky, W. (1968). Human brain: left-right asymmetries in temporal speech region. Science, 161(3837), 186-187.

Gomez-Robles, A., Hopkins, W. D., & Sherwood, C. C. (2013). Increased morphological asymmetry, evolvability and plasticity in human brain evolution. Proc Biol Sci, 280(1761), 20130575. doi:10.1098/rspb.2013.0575

Good, C. D., Johnsrude, I., Ashburner, J., Henson, R. N., Friston, K. J., & Frackowiak, R. S. (2001). Cerebral asymmetry and the effects of sex and handedness on brain structure: a voxel-based morphometric analysis of 465 normal adult human brains. Neuroimage, 14(3), 685-700. doi:10.1006/nimg.2001.0857

Greve, D. N., Van der Haegen, L., Cai, Q., Stufflebeam, S., Sabuncu, M. R., Fischl, B., & Brysbaert, M. (2013). A surface-based analysis of language lateralization and cortical asymmetry. J Cogn Neurosci, 25(9), 1477-1492. doi:10.1162/jocn_a_00405

Guadalupe, T., Willems, R. M., Zwiers, M. P., Arias Vasquez, A., Hoogman, M., Hagoort, P., Francks, C. (2014). Differences in cerebral cortical anatomy of left- and right-handers. Front Psychol, 5, 261. doi:10.3389/fpsyg.2014.00261

Holloway, R. L., & De La Costelareymondie, M. C. (1982). Brain endocast asymmetry in pongids and hominids: some preliminary findings on the paleontology of cerebral dominance. Am J Phys Anthropol, 58(1), 101-110. doi:10.1002/ajpa.1330580111

Hopkins, W. D., & Avants, B. B. (2013). Regional and hemispheric variation in cortical thickness in chimpanzees (*Pan* troglodytes). J Neurosci, 33(12), 5241-5248. doi:10.1523/jneurosci.2996-12.2013

Hopkins, W. D., & Cantalupo, C. (2004). Handedness in chimpanzees (Pan troglodytes) is associated with asymmetries of the primary motor cortex but not with homologous language areas. Behav Neurosci, 118(6), 1176-1183. doi:10.1037/0735-7044.118.6.1176

Hopkins, W. D., Li, X., Crow, T., & Roberts, N. (2016). Vertex- and atlas-based comparisons in measures of cortical thickness, gyrification and white matter volume between humans and chimpanzees. Brain Struct Funct. doi:10.1007/s00429-016-1213-1

Hopkins, W. D., & Marino, L. (2000). Asymmetries in cerebral width in nonhuman primate brains as revealed by magnetic resonance imaging (MRI). Neuropsychologia, 38(4), 493-499.

Hopkins, W. D., Misiura, M., Pope, S. M., & Latash, E. M. (2015). Behavioral and brain asymmetries in primates: a preliminary evaluation of two evolutionary hypotheses. Ann N Y Acad Sci, 1359, 65-83. doi:10.1111/nyas.12936

Hopkins, W. D., & Nir, T. (2010). Planum temporale surface area and grey matter asymmetries in chimpanzees (*Pan* troglodytes): The effect of handedness and comparison within findings in humans. Behavioural Brain Research, 208(2), 436-443.

Ide, A., Rodriguez, E., Zaidel, E., & Aboitiz, F. (1996). Bifurcation patterns in the human Sylvian fissure:hemispheric and sex differences. Cerebral Cortex, 6(5), 717-725.

Josse, G., Kherif, G., Flandin, G., Seghier, M. L., & Price, C. J. (2009). Predicting language lateralization from gray matter. Journal of Neuroscience, 29(43), 13516-13523.

Keller, S. S., Deppe, M., Herbin, M., & Gilissen, E. (2012). Variability and asymmetry of the sulcal contours defining Broca's area homologue in the chimpanzee brain. J Comp Neurol, 520(6), 1165-1180. doi:10.1002/cne.22747

Keller, S. S., Highley, J. R., Garcia-Finana, M., Sluming, V., Rezaie, R., & Roberts, N. (2007). Sulcal variability, stereological measurement and asymmetry of Broca's area on MR images. *J Anat, 211*(4), 534-555. doi:10.1111/j.1469-7580.2007.00793.x

Knecht, S., Drager, B., Deppe, M., Bobe, L., Lohmann, H., Floel, A., Henningsen, H. (2000). Handedness and hemispheric language dominance in healthy humans. Brain, 123(12), 2512-2518.

Koelkebeck, K., Miyata, J., Kubota, M., Kohl, W., Son, S., Fukuyama, H., Murai, T. (2014). The contribution of cortical thickness and surface area to gray matter asymmetries in the healthy human brain. Hum Brain Mapp, *35*(12), 6011-6022. doi:10.1002/hbm.22601

Kong, X. Z., Mathias, S. R., Guadalupe, T., Glahn, D. C., Franke, B., Crivello, F., Francks, C. (2018). Mapping cortical brain asymmetry in 17,141 healthy individuals worldwide via the ENIGMA Consortium. Proc Natl Acad Sci U S A, 115(22), E5154-e5163. doi:10.1073/pnas.1718418115

Le Guen, Y., Auzias, G., Leroy, F., Noulhiane, M., Dehaene-Lambertz, G., Duchesnay, E., Frouin, V. (2018a). Genetic Influence on the Sulcal Pits: On the Origin of the First Cortical Folds. Cereb Cortex, 28(6), 1922-1933. doi:10.1093/cercor/bhx098

Le Guen, Y., Leroy, F., Auzias, G., Riviere, D., Grigis, A., Mangin, J. F., Frouin, V. (2018b). The chaotic morphology of the left superior temporal sulcus is genetically constrained. Neuroimage, *174*, 297-307. doi:10.1016/j.neuroimage.2018.03.046

LeMay, M. (1982). Morphological aspects of human brain asymmetry: An evolutionary perspective. Trends in Neurosciences, 5, 273-275.

Leroy, F., Cai, Q., Bogart, S. L., Dubois, J., Coulon, O., Monzalvo, K., Dehaene-Lambertz, G. (2015). New human-specific brain landmark: the depth asymmetry of superior temporal sulcus. Proc Natl Acad Sci U S A, 112(4), 1208-1213. doi:10.1073/pnas.1412389112

Luders, E., Narr, K. L., Thompson, P. M., Rex, D. E., Jancke, L., & Toga, A. W. (2006). Hemispheric asymmetries in cortical thickness. Cereb Cortex, 16(8), 1232-1238. doi:10.1093/cercor/bhj064

Lyall, A. E., Shi, F., Geng, X., Woolson, S., Li, G., Wang, L., Gilmore, J. H. (2015). Dynamic Development of Regional Cortical Thickness and Surface Area in Early Childhood. Cereb Cortex, 25(8), 2204-2212. doi:10.1093/cercor/bhu027

Lyn, H. L., Pierre, P., Bennett, A. J., Fears, S. C., Woods, R. P., & Hopkins, W. D. (2011). Planum temporale grey matter asymmetries in chimpanzees (*Pan* troglodytes), vervet (Chlorocebus aethiops sabaeus), rhesus (Macaca mulatta) and bonnet (Macaca radiata) monkeys. Neuropsychologia, 49, 2004-2012.

Lyttelton, O. C., Karama, S., Ad-Dab'bagh, Y., Zatorre, R. J., Carbonell, F., Worsley, K., & Evans, A. C. (2009). Positional and surface area asymmetry of the human cerebral cortex. Neuroimage, *46*(4), 895-903. doi:10.1016/j.neuroimage.2009.03.063

Maingault, S., Tzourio-Mazoyer, N., Mazoyer, B., & Crivello, F. (2016). Regional correlations between cortical thickness and surface area asymmetries: A surface-based morphometry study of 250 adults. Neuropsychologia, 93(Pt B), 350-364. doi:10.1016/j.neuropsychologia.2016.03.025

Marie, D., Roth, M., Lacoste, R., Nazarian, B., Bertello, A., Anton, J. L., Meguerditchian, A. (2017). Left Brain Asymmetry of the Planum Temporale in a Nonhominid Primate: Redefining the Origin of Brain Specialization for Language. Cereb Cortex, 1-8. doi:10.1093/cercor/bhx096

Meyer, M., Liem, F., Hirsiger, S., Jancke, L., & Hanggi, J. (2014). Cortical surface area and cortical thickness demonstrate differential structural asymmetry in auditory-related areas of the human cortex. Cereb Cortex, 24(10), 2541-2552. doi:10.1093/cercor/bht094

Ocklenburg, S., & Gunturkun, O. (2018). The Lateralized Brain: The Neuroscience and Evolution of Hemispheric Asymmetries. London: Academic Press.

Panizzon, M. S., Fennema-Notestine, C., Eyler, L. T., Jernigan, T. L., Prom-Wormley, E., Neale, M., Kremen, W. S. (2009). Distinct genetic influences on cortical surface area and cortical thickness. Cereb Cortex, 19(11), 2728-2735. doi:10.1093/cercor/bhp026

Plessen, K. J., Hugdahl, K., Bansal, R., Hao, X., & Peterson, B. S. (2014). Sex, age, and cognitive correlates of asymmetries in thickness of the cortical mantle across the life span. J Neurosci, 34(18), 6294-6302. doi:10.1523/jneurosci.3692-13.2014

Rakic, P. (1995). A small step for the cell, a giant leap for mankind: a hypothesis of neocortical expansion during evolution. Trends Neurosci, 18(9), 383-388.

Rilling, J. K., Glasser, M. F., Jbabdi, S., Andersson, J., & Preuss, T. M. (2011). Continuity, divergence, and the evolution of brain language pathways. Front Evol Neurosci, 3, 11. doi:10.3389/fnevo.2011.00011

Rogers, L. J., Vallortigara, G., & Andrew, R. J. (2013). Divided brains: the biology and behaviour of brain asymmetries. New York: Cambridge University Press.

Rubens, A. B., Mahowald, M. W., & Hutton, J. T. (1976). Asymmetry of the lateral (Sylvian) fissures in man. Neurology, 26(7), 620-624.

Savic, I. (2014). Asymmetry of cerebral gray and white matter and structural volumes in relation to sex hormones and chromosomes. Front Neurosci, 8, 329. doi:10.3389/fnins.2014.00329

Shapleske, J., Rossell, S. L., Woodruff, P. W., & David, A. S. (1999). The planum temporale: a systematic, quantitative review of its structural, functional and clinical significance. Brain Research Reviews, 29, 26-49.

Sherwood, C. C., Wahl, E., Erwin, J. M., Hof, P. R., & Hopkins, W. D. (2007). Histological asymmetries of primary motor cortex predict handedness in chimpanzees (*Pan* troglodytes). *J Comp Neurol, 503*(4), 525-537. doi:10.1002/cne.21399

Takaya, S., Kuperberg, G. R., Liu, H., Greve, D. N., Makris, N., & Stufflebeam, S. M. (2015). Asymmetric projections of the arcuate fasciculus to the temporal cortex underlie lateralized language function in the human brain. Front Neuroanat, 9, 119. doi:10.3389/fnana.2015.00119

Trivedi, R., Agarwal, S., Rathore, R. K., Saksena, S., Tripathi, R. P., Malik, G. K., Gupta, R. K. (2009). Understanding development and lateralization of major cerebral fiber bundles in pediatric population through quantitative diffusion tensor tractography. Pediatr Res, 66(6), 636-641. doi:10.1203/PDR.0b013e3181bbc6b5

Vadlamudi, L., Hatton, R., Byth, K., Harasty, J., Vogrin, S., Cook, M. J., & Bleasel, A. F. (2006). Volumetric analysis of a specific language region- the planum temporale. Journal of Clinical Neuroscience, 13, 206-213.

Van Essen, D. C., Glasser, M. F., Dierker, D. L., Harwell, J., & Coalson, T. (2012). Parcellations and hemispheric asymmetries of human cerebral cortex analyzed on surface-based atlases. Cereb Cortex, 22(10), 2241-2262. doi:10.1093/cercor/bhr291

Vuoksimaa E, Panizzon MS, Chen CH, Fiecas M, Eyler LT, Fennema-Notestine C, Hagler DJ, Fischl B, Franz CE, Jak A et al. 2015. The genetic association between neocortical volume and general cognitive ability is driven by global surface area rather than thickness. Cereb Cortex. 25(8):2127-2137.

Watkins, K. E., Paus, T., Lerch, J. P., Zijdenbos, A., Collins, D. L., Neelin, P., Taylor, J., Worsley, K. J., Evans, A. C. 2001. Structural asymmetries in the human brain: A voxel-based statistical analysis of 142 MRI scans. Cereb Cortex. 11(9):868-877.

Wiberg, A., Ng, M., Al Omran, Y., Alfaro-Almagro, F., McCarthy, P., Marchini, J., Furniss, D. (2019). Handedness, language areas and neuropsychiatric diseases: insights from brain imaging and genetics. Brain, 142(10), 2938-2947. doi:10.1093/brain/awz257

Winkler, A. M., Kochunov, P., Blangero, J., Almasy, L., Zilles, K., Fox, P. T., Glahn, D. C. (2010). Cortical thickness or grey matter volume? The importance of selecting the phenotype for imaging genetics studies. Neuroimage, 53(3), 1135-1146. doi:10.1016/j.neuroimage.2009.12.028

Witelson, S., & Kigar, D. (1988). Asymmetry of brain function follows asymmetry in anatomical form: gross, microscopic, postmortem and imaging studies. In: Boller, Grafman, J. (Eds.), Handbook of Neuropsychology (pp. 111–142): Elsevier.

Xiang, L., Crow, T., & Roberts, N. (2019a). Automatic analysis of cross-sectional cerebral asymmetry on 3D in vivo MRI scans of human and chimpanzee. J Neurosci Res. doi:10.1002/jnr.24391

Xiang, L., Crow, T., & Roberts, N. (2019b). Cerebral torque is human specific and unrelated to brain size. Brain Struct Funct. doi:10.1007/s00429-018-01818-0

Xiang, L., Crow, T. J., Hopkins, W. D., Gong, Q., & Roberts, N. (2018). Human torque is not present in chimpanzee brain. Neuroimage, 165, 285-293. doi:10.1016/j.neuroimage.2017.10.017

Yeni-Komshian, G., & Benson, D. (1976). Anatomical study of cerebral asymmetry in the temporal lobe of humans, chimpanzees and monkeys. Science, 192, 387-389.

Zhou, D., Lebel, C., Evans, A., & Beaulieu, C. (2013). Cortical thickness asymmetry from childhood to older adulthood. Neuroimage, 83, 66-74. doi:10.1016/j.neuroimage.2013.06.073

Zilles, K., Dabringhaus, A., Geyer, S., Amunts, K., Qu, M., Schleicher, A., Steinmetz, H. (1996). Structural asymmetries in the human forebrain and the forebrain of non-human primates and rats. Neuroscience and Biobehavioral Reviews, 20, 593-605.

Tables

	Methods and Measurements	Main findings of the study
Lyttelton et al. (2009), 112 right-handed human subjects	SBM-based vertex-wise analysis of SA and positional asymmetry	SA asymmetry to the left in the supra-marginal gyrus, Heschl's gyrus, PT, anterior superior temporal, lateral orbital frontal cortex and to the right in the anterior occipital lobe, dorsal anterior cingulate and medial orbital frontal; positional asymmetry in the pattern cerebral torque
Zhou et al. (2013), 274 right-handed human subjects	SBM-based vertex-wise analysis of CT asymmetry	CT asymmetry emerges extensively after adolescence and develops more pronounced with age
Maingault et al. (2016), 250 human subjects (120 left-handers)	SBM-based vertex-wise analysis of GMV, SA, CT and sulcal depth asymmetry	Global GMV, SA and CT asymmetry to the right; no significant correlation between the global SA and CT asymmetry; handedness is not associated with cortical asymmetries
Meyer et al. (2014), 104 healthy human subjects	Destrieux atlas-based ROI analysis of GMV, SA and CT asymmetry	Global rightward asymmetry in GMV and SA but not CT; leftward SA asymmetry in auditory-related cortex and rightward CT asymmetry in the primary and secondary auditory cortex
Koelkebeck et al. (2014), 101 right-handed human subjects	Desikan-Killiany atlas-based ROI analysis of GMV, SA and CT asymmetry	Different patterns of asymmetry in different measures; more prominent SA asymmetry compared to CT asymmetry
Chiarello et al. (2016), 200 healthy human subjects	Destrieux atlas-based ROI analysis of SA, CT and LGI asymmetry	Extensive asymmetries of all three measures; substantial differences between different measures in both pattern and extent; regions with larger between-subject variability also show greater asymmetry
Kong et al. (2018), 17,141 healthy human subjects	Desikan-Killiany atlas-based ROI analysis of SA, CT asymmetry	Global rightward asymmetry in SA and leftward asymmetry in CT; substantial and differential regional asymmetry in SA and CT which interacts with sex, age and ICV; no overall correlation between SA and CT asymmetry; handedness is not associated with cortical asymmetries
Guen et al. (2018b), 800+ subjects from the Human Connectome Project (HCP)	Novel ROI-based analysis of sulcal pit distribution asymmetry	Sulcal pit asymmetry in the STS to be genetically determined

Table 1. Studies of cerebral asymmetry in the human brain.

		Human		Chimpanzee	
Hemisphere		**SA (x1.0e+05 mm^2)**	**CT (mm)**	**SA (x1.0e+04 mm^2)**	**CT (mm)**
Left		1.11 ± 0.11	2.29 ± 0.09	3.67 ± 0.29	1.39 ± 0.11
Right		1.12 ± 0.11	2.30 ± 0.09	3.68 ± 0.29	1.40 ± 0.12
Asymmetry	**t-stat**	-3.82	-1.10	-0.39	-1.31
	p-value (2-tailed)	< 0.001	0.27	0.70	0.19

Table 2. Statistics of the global SA and CT values for the human and chimpanzee brain showing (i) significant rightward SA asymmetry in the human brain but not for CT, and (ii) no significant asymmetry for either SA or CT in the chimpanzee brain.

Surface Area	Human		Chimpanzee		Species Difference	
ROIs	**AI**	**p-value**	**AI**	**p-value**	**t-stats**	**p-value**
Frontal						
Superior frontal	-0.02	-0.03*	0.01	0.40	-2.14	0.03*
Rostral middle frontal	-0.02	-0.04*	-0.01	-0.46	-0.59	0.56
Caudal middle frontal	0.01	0.68	0.01	0.68	0.08	0.93
Pars-opercularis	0.01	0.51	0.00	0.90	0.41	0.68
Pars-triangularis	0.02	0.12	-0.00	-0.85	1.04	0.30
Pars-orbitalis	0.01	0.32	-0.02	-0.45	1.17	0.24
Lateral orbito frontal	0.01	0.13	0.03	0.10	-1.06	0.29
Medial orbito frontal	-0.09	-0.00**	0.01	0.78	-2.81	0.01*
Precentral	-0.01	-0.06	-0.01	-0.15	-0.58	0.56
Paracentral	0.01	0.36	-0.02	-0.02*	1.72	0.09
Frontal pole	-0.02	-0.13	0.00	0.83	-1.28	0.20
Parietal						
Superior parietal	-0.03	-0.002*	0.01	0.37	-2.91	0.00*
Inferior parietal	-0.05	-0.00**	-0.00	-0.79	-3.80	0.00**
Supramarginal	0.10	0.00**	0.01	0.10	5.47	0.00**
Postcentral	0.03	0.00**	-0.00	-0.68	3.25	0.00**
Precuneus	-0.01	-0.16	-0.01	-0.51	-0.30	0.76
Temporal						
Middle temporal	-0.00	-0.58	0.01	0.39	-1.03	0.30
Inferior temporal	0.04	0.00**	0.01	0.31	1.86	0.06
Superior temporal	0.02	0.03*	0.03	0.00**	-1.68	0.10
Bankssts	-0.05	-0.02*	-0.01	-0.17	-1.43	0.15
Fusiform	-0.00	-0.97	0.01	0.34	-0.81	0.42
Transverse temporal	0.07	0.00**	0.02	0.04*	2.53	0.01*
Entorhinal	-0.02	-0.23	-0.06	-0.13	0.83	0.41
Temporal pole	0.07	0.00**	0.02	0.37	1.93	0.05
Parahippocampal	-0.00	-0.96	-0.02	-0.50	0.61	0.54
Occipital						
Lateral occipital	-0.01	-0.24	-0.02	-0.08	0.53	0.60
Lingual	-0.03	-0.01*	-0.00	-0.88	-1.35	0.18
Cuneus	-0.09	-0.00**	0.08	0.00**	-7.04	0.00**
Pericalcarine	-0.06	-0.00**	0.00	0.99	-2.27	0.02*
Cingulate & Insula						
Caudal anterior cingulate	-0.09	-0.003*	0.05	0.02*	-3.69	0.00**
Isthmus cingulate	0.07	0.00**	-0.00	-0.99	2.16	0.03*
Posterior cingulate	-0.03	-0.02*	0.01	0.70	-1.95	0.05
Rostral anterior cingulate	0.02	0.32	0.16	0.03*	-1.36	0.18
Insula	-0.01	0.10	0.00	0.51	-1.33	0.19

Table 3. Statistics of ROI-based SA asymmetry for the human and chimpanzee brain. * denotes ROI's with significant asymmetry (i.e. $p < 0.05$ uncorrected for multiple comparisons), and ** denotes ROI's with highly significant asymmetry that survived the Bonferroni correction (i.e. $p < 0.05/34$).

Cortical Thickness	Human		Chimpanzee		Species Difference	
ROIs	**AI**	**p-value**	**AI**	**p-value**	**t-stats**	**p-value**
Frontal						
Superior frontal	0.02	0.00**	-0.00	-0.94	4.75	0.00**
Rostral middle frontal	0.03	0.00**	0.02	0.01*	0.95	0.34
Caudal middle frontal	0.00	0.34	-0.01	-0.45	1.20	0.23
Pars-opercularis	0.00	0.38	0.00	0.87	0.38	0.70
Pars-triangularis	-0.00	-0.61	0.01	0.31	-1.16	0.25
Pars-orbitalis	-0.02	-0.08	-0.01	-0.31	-0.29	0.78
Lateral orbito frontal	0.01	0.16	-0.01	-0.11	2.15	0.03*
Medial orbito frontal	0.00	0.93	-0.01	-0.41	0.72	0.47
Precentral	0.00	0.61	-0.03	-0.00**	3.84	0.00**
Paracentral	-0.02	-0.005*	-0.04	-0.00**	2.21	0.03*
Frontal pole	0.02	0.07	0.00	0.99	1.10	0.27
Parietal						
Superior parietal	0.01	0.14	-0.00	-0.42	1.58	0.12
Inferior parietal	-0.01	-0.02*	-0.00	-0.65	-0.94	0.35
Supramarginal	0.00	0.69	0.01	0.03*	-1.33	0.18
Postcentral	0.01	0.05	-0.00	-0.28	2.19	0.03*
Precuneus	-0.00	-0.98	0.03	0.00**	-3.67	0.00**
Temporal						
Middle temporal	-0.02	-0.00**	0.01	0.06	-3.88	0.00**
Inferior temporal	-0.02	-0.00**	-0.00	-0.81	-2.02	0.04*
Superior temporal	-0.02	-0.002*	-0.00	-0.64	-1.67	0.10
Bankssts	-0.03	-0.00*	0.00	0.83	-2.09	0.04*
Fusiform	-0.01	-0.03*	-0.01	-0.26	-0.26	0.79
Transverse temporal	-0.01	-0.55	-0.03	-0.01*	1.83	0.07
Entorhinal	-0.02	-0.06	-0.00	-0.83	-0.86	0.39
Temporal pole	-0.00	-0.75	-0.01	-0.71	0.16	0.88
Parahippocampal	-0.02	-0.01*	-0.04	-0.00**	1.28	0.20
Occipital						
Lateral occipital	-0.03	-0.00**	-0.02	-0.00**	-1.27	0.21
Lingual	-0.04	-0.00**	-0.01	-0.16	-3.26	0.00**
Cuneus	-0.03	-0.00**	0.00	0.97	-3.63	0.00**
Pericalcarine	-0.04	-0.00**	0.01	0.38	-3.70	0.00**
Cingulate & insula						
Caudal anterior cingulate	0.01	0.38	0.06	0.00**	-2.54	0.01*
Isthmus cingulate	-0.00	-0.97	-0.02	-0.08	1.33	0.18
Posterior cingulate	0.01	0.11	0.00	0.62	0.68	0.50
Rostral anterior cingulate	0.06	0.00**	0.05	0.01*	0.53	0.60
Insula	0.00	0.49	0.02	0.00**	-2.52	0.01*

Table 4. Statistics of ROI-based CT asymmetry index for the human and chimpanzee brain. * denotes ROI's with significant asymmetry (i.e. $p < 0.05$ uncorrected for multiple comparisons), and ** denotes ROI's with highly significant asymmetry that survived the Bonferroni correction (i.e. $p < 0.05/34$).

Figure Captions

Figure 1. Flow diagrams of the steps in the application of the single atlas parcellation scheme (SAPS), and two atlas parcellation scheme (TAPS), for vertex-wise (a and c) and ROI-based analyses (b and d) are shown in the left and right columns, respectively, for the case of an individual in the chimpanzee cohort. For the vertex-wise analysis in SAPS (a) the inter-hemispheric and between subject correspondences are established by co-registering both cerebral hemispheres of individual subjects to a symmetric registration atlas. For the corresponding vertex-wise analysis in TAPS (b) only between subject correspondences are established by separately co-registering left and right cerebral hemispheres of individual subjects to the relevant side of the atlas. For ROI-based analysis in SAPS (c) the parcellation of one cerebral hemisphere of the Desikan-Killiany atlas (e.g. left side) is first projected to both the ipsilateral and contralateral cerebral hemisphere of individual subjects. The pipeline is then repeated using the opposite side of the Desikan-Killiany atlas and the two results are averaged. For ROI-based analysis in TAPS (d) the parcellation convention of each cerebral hemisphere in the Desikan-Killiany atlas is propagated separately to the corresponding hemisphere of individual subjects. The illustration is simplified by showing only one half of the SAPS analysis pipeline for step-by-step comparison with TAPS.

Figure 2. Vertex-wise results of (a) SA and (b) CT asymmetry illustrating (i) significant asymmetries for the human (left) and chimpanzee brain (right), in which hot colours refer to leftward asymmetry and cool colours to rightward asymmetry and (ii) significant difference of asymmetry between the human and chimpanzee brain (middle), in which the intensity of the hot colour indicates the significance level of the difference. The highlighted areas survive the cluster-wise correction for multiple comparisons and the significance level of the respective cluster forming, and cluster-wise alphas are set as $p < 0.01$.

Figure 3. ROI-based results of (a) SA and (b) CT asymmetry illustrating (i) significant signed asymmetries across 34 ROIs for the human (left panel) and (ii) chimpanzee brain (right panel), in which hot colours refer to leftward asymmetry and cool colours to rightward asymmetry, and (iii) difference between species (middle panel), in which the intensity of the hot colour

indicates the significance level of the difference. Bonferroni correction is performed in ROI-based analysis and the significance level is set as $p < 0.05/34$.

Figure 4. Vertex-wise average asymmetry maps of (a) SA and (b) CT. In each panel, the left shows the result for the human brain and right for the chimpanzee brain. Hot colours correspond to leftward asymmetry and cool colours to rightward asymmetry. The yellow contours are drawn to identify regions of significant species difference.

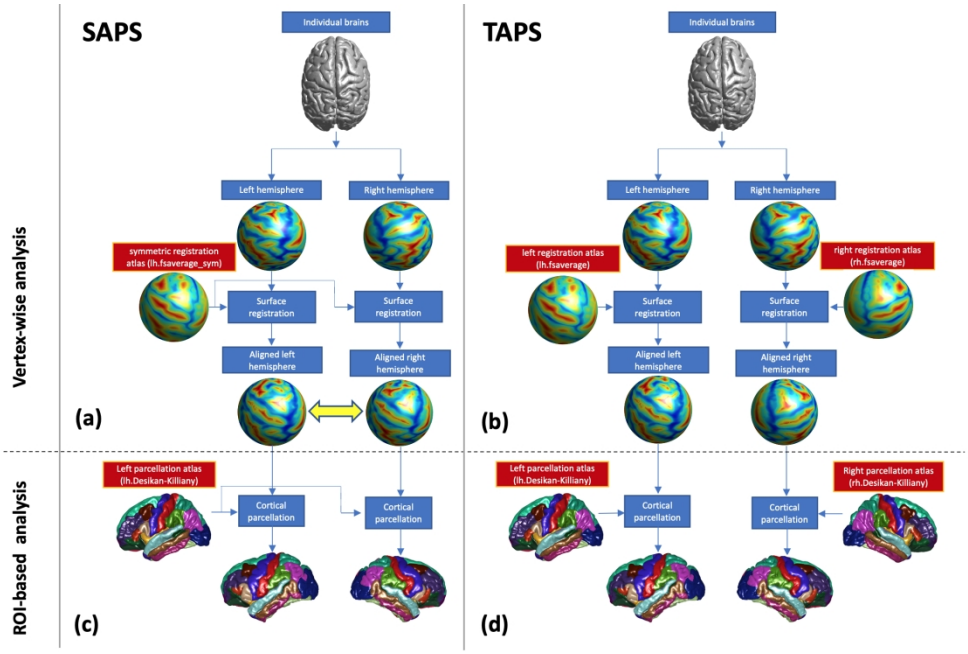

Figure 1. Flow diagrams of the steps in the application of the single atlas parcellation scheme (SAPS), and two atlas parcellation scheme (TAPS), for vertex-wise (a and c) and ROI-based analyses (b and d) are shown in the left and right columns, respectively, for the case of an individual in the chimpanzee cohort. For the vertex-wise analysis in SAPS (a) the inter-hemispheric and between subject correspondences are established by co-registering both cerebral hemispheres of individual subjects to a symmetric registration atlas. For the corresponding vertex-wise analysis in TAPS (b) only between subject correspondences are established by separately co-registering left and right cerebral hemispheres of individual subjects to the relevant side of the atlas. For ROI-based analysis in SAPS (c) the parcellation of one cerebral hemisphere of the Desikan-Killiany atlas (e.g. left side) is first projected to both the ipsilateral and contralateral cerebral hemisphere of individual subjects. The pipeline is then repeated using the opposite side of the Desikan-Killiany atlas and the two results are averaged. For ROI-based analysis in TAPS (d) the parcellation convention of each cerebral hemisphere in the Desikan-Killiany atlas is propagated separately to the corresponding hemisphere of individual subjects. The illustration is simplified by showing only one half of the SAPS analysis pipeline for step-by-step comparison with TAPS.

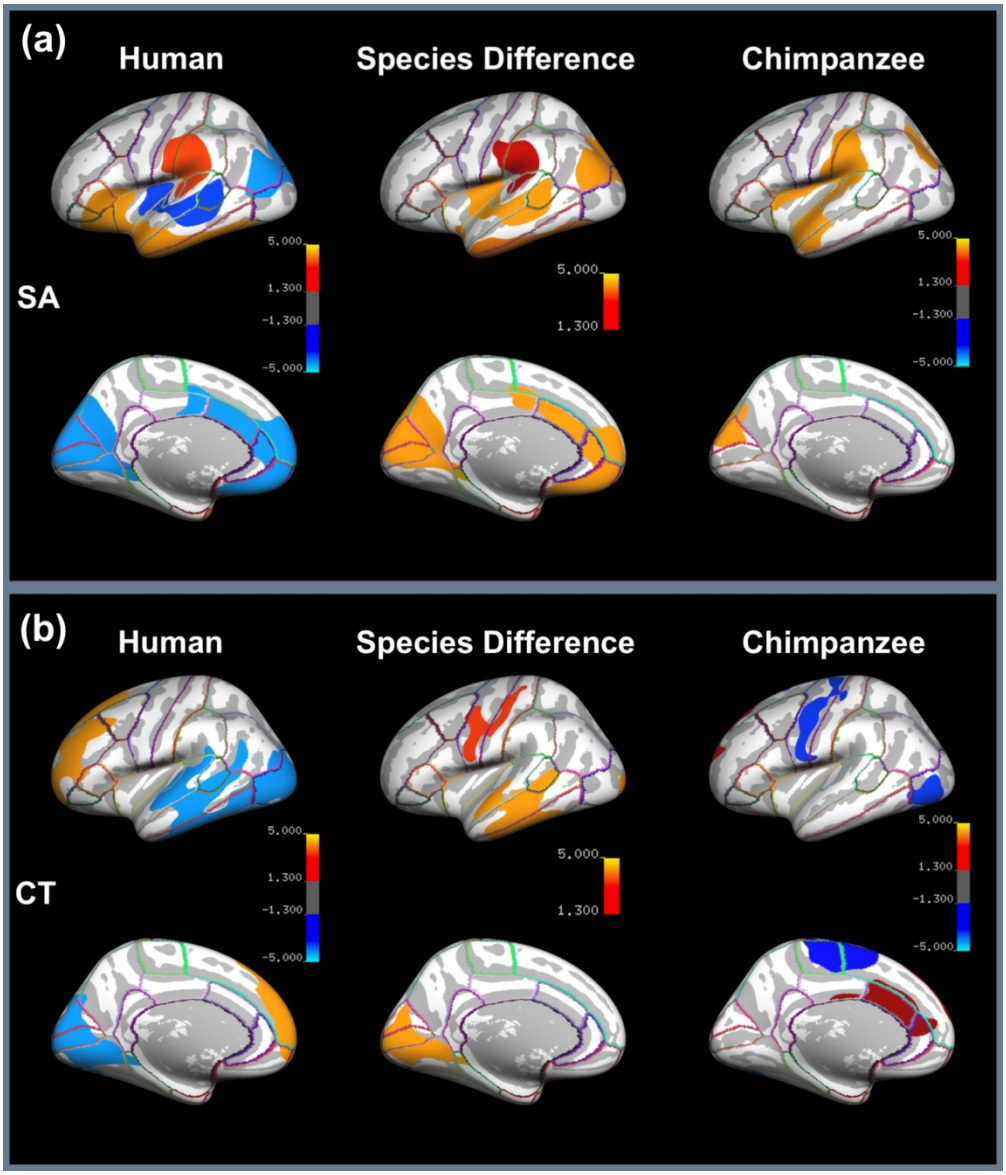

Figure 2. Vertex-wise results of (a) SA and (b) CT asymmetry illustrating (i) significant asymmetries for the human (left) and chimpanzee brain (right), in which hot colours refer to leftward asymmetry and cool colours to rightward asymmetry and (ii) significant difference of asymmetry between the human and chimpanzee brain (middle), in which the intensity of the hot colour indicates the significance level of the difference. The highlighted areas survived the cluster-wise correction for multiple comparisons and the significance level of the respective cluster forming, and cluster-wise alphas are set as $p < 0.01$.

643x750mm (72 x 72 DPI)

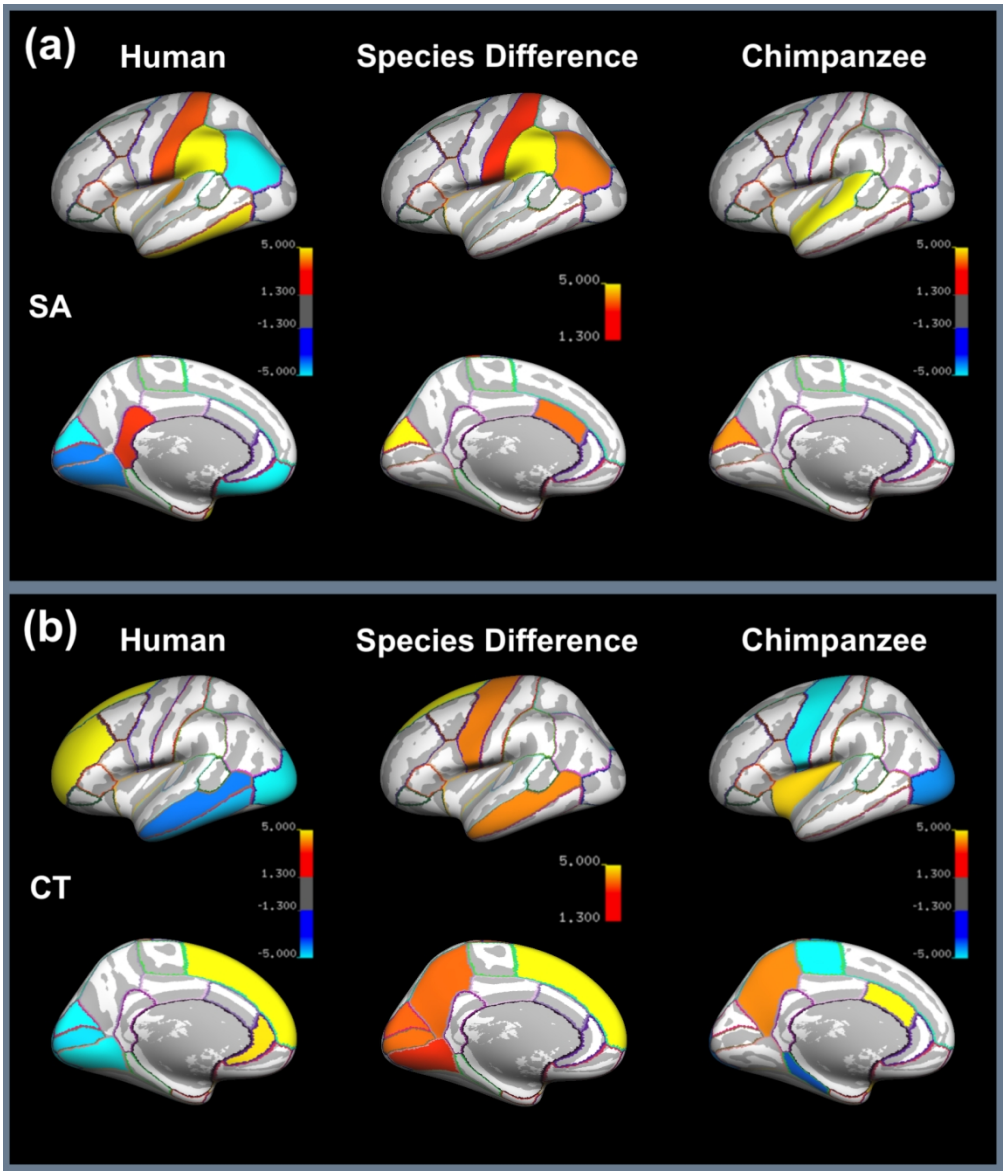

Figure 3. ROI-based results of (a) SA and (b) CT asymmetry illustrating (i) significant asymmetries across 34 ROIs for the human (left panel) and (ii) chimpanzee brain (right panel), in which hot colours refer to leftward asymmetry and cool colours to rightward asymmetry, and (iii) difference between species (middle panel), in which the intensity of the hot colour indicates the significance level of the difference. Bonferroni correction is performed in ROI-based analysis and the significance level is set as $p < 0.05/34$.

643x750mm (72 x 72 DPI)

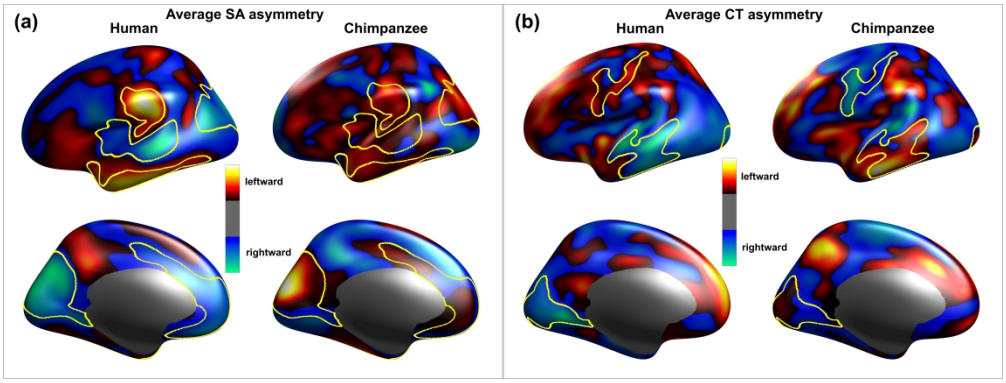

Figure 4. Vertex-wise average asymmetry maps of (a) SA and (b) CT. In each panel, the left shows the result for the human brain and right for the chimpanzee brain. Hot colours correspond to leftward asymmetry and cool colours to rightward asymmetry. The yellow contours are drawn to identify regions of significant species difference.

SUPPLEMENTARY MATERIALS

1 Evaluation of the effect of atlas-bias on ROI-based analysis of SA asymmetry

The FreeSurfer parcellation atlas, i.e. Desikan-Killiany atlas (Desikan et al., 2006) is asymmetric between the left and right cerebral hemisphere (see Figure S1 (a)). Being constructed by averaging the manual delineations of 34 ROIs that are defined by relevant gyri for each cerebral hemisphere on co-registered 3D MRI scans obtained for 40 individuals, the neuro-anatomical atlas carries the inherent asymmetry of the human brain. According to Figure S1 (b), significantly different numbers of vertices are assigned to corresponding ROIs of the left and right cerebral hemispheres of the Desikan-Killiany atlas, i.e., the inter-hemispheric difference is greater than 10% in ten regions, namely, caudal anterior cingulate, inferior parietal, transverse temporal, entorhinal, middle temporal, paracentral, pars-opercularis, pars-triangularis, rostral anterior cingulate and frontal pole. We hypothesised that the asymmetry in the atlas can cause systematic bias in the computation of brain asymmetry for individual subjects through differential distribution of vertices during the parcellation process if the conventional two-atlas based parcellation scheme (TAPS) is applied. An experiment was conducted to apply the Desikan-Killiany atlas to compute brain asymmetry using TAPS and SAPS, respectively. Specially, we randomly selected 3D MR images for 14 subjects from the human cohort and prepared a corresponding series of images for the same subjects which however, had been left-right flipped with respect to plane x=0 in the MNI space. The results of the average brain asymmetry for the original brain scans and their mirror reflections using the two schemes are shown in Figure S2.

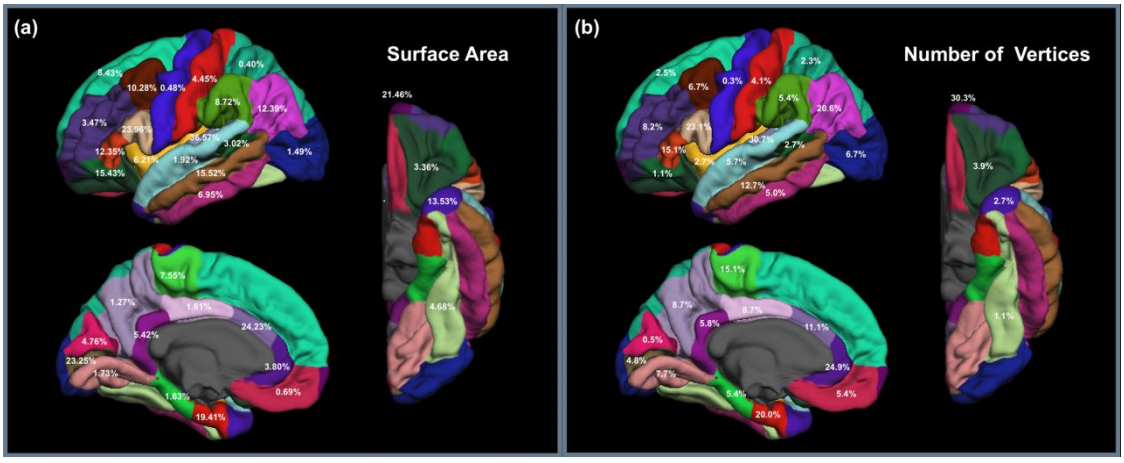

Figure S1. Atlas-bias computed as the normalized difference of (a) surface area and (b) number of vertices between corresponding ROIs of the left and right cerebral hemisphere.

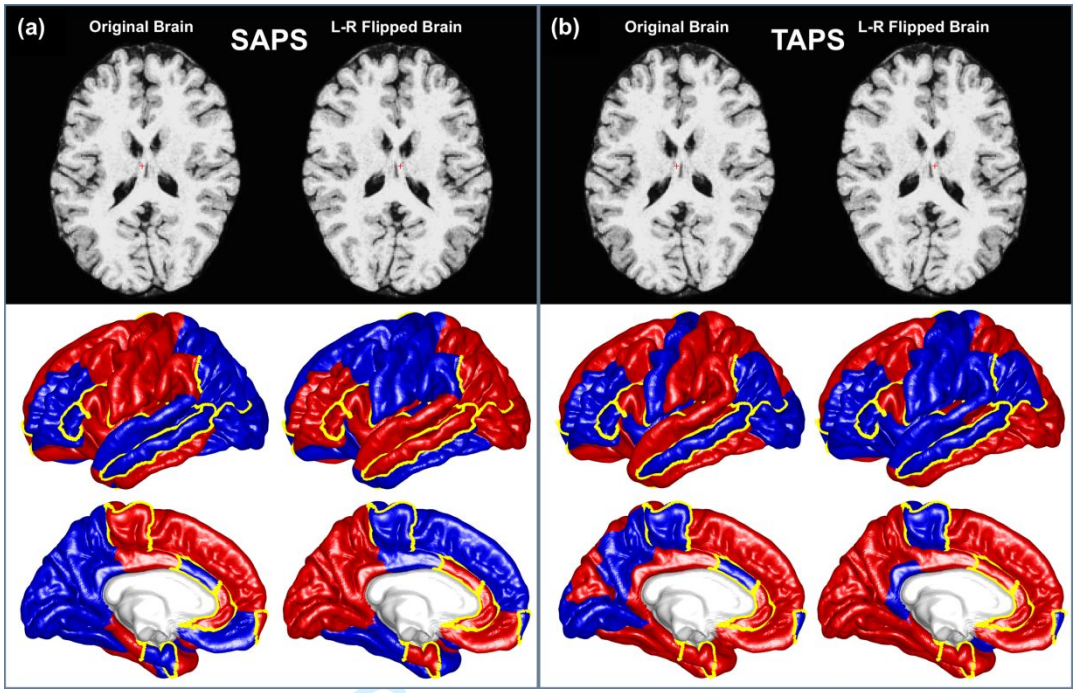

Figure S2. Results of SA asymmetry computed based on (a) SAPS in the present study and (b) TAPS in FreeSurfer illustrating the former provides more accurate and reliable results than the latter. In each panel, the top row demonstrates the orientation of the brain scan and the bottom shows the corresponding SA asymmetry; the left refers to average SA asymmetry of the brain images of 14 human subjects and the right refers to average SA asymmetry for the same 14 brain images analysed with the same respective atlas after being flipped left-right with respect to plane x=0 in the MNI space. Red colour denotes leftward asymmetry and blue colour rightward asymmetry. The regions with large inter-hemispheric parcellation difference (i.e. greater than 10%) are highlighted using yellow contour (see also Figure S1 (b)).

2 Regional parcellation for the chimpanzee brain

Examples for 10 randomly selected chimpanzee subjects are shown in Figure S3, which demonstrate that the Desikan-Killiany atlas provides reasonable parcellation results for the chimpanzee brain.

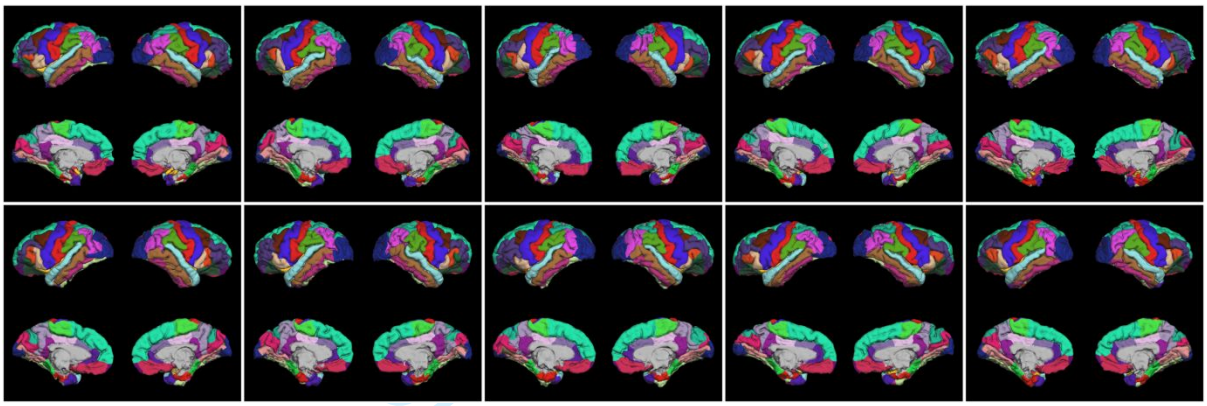

Figure S3. The automatic cortical parcellation for 10 brains randomly selected from the chimpanzee cohort demonstrating excellent correspondence between the boundaries of the ROIs propagated from the human Desikan-Killiany atlas.

3 ROI-based cortical measurements for the human and chimpanzee brains

Surface Area	Human				Chimpanzee			
ROIs	Left Hemisphere		Right Hemisphere		Left Hemisphere		Right Hemisphere	
	mean	SD	mean	SD	mean	SD	mean	SD
Frontal								
Superior frontal	9160.20	1215.23	9312.63	1187.96	2822.15	242.25	2806.18	241.21
Rostral middle frontal	7683.78	1095.67	7844.30	1168.82	1772.58	244.74	1792.42	267.16
Caudal middle frontal	2743.60	506.44	2717.71	481.18	854.05	102.75	848.92	103.13
Pars-opercularis	2188.76	373.04	2169.89	392.17	693.75	99.51	693.84	109.61
Pars-triangularis	1896.33	289.30	1856.14	314.18	497.73	109.06	500.65	112.94
Pars-orbitalis	1181.31	126.01	1172.71	156.98	234.46	34.74	239.04	41.22
Lateral orbito frontal	3421.74	464.57	3383.83	454.92	1042.83	284.75	1007.88	285.93
Medial orbito frontal	2778.06	400.27	3089.12	767.53	1482.83	571.62	1480.29	622.98
Precentral	5659.86	683.81	5745.99	707.24	2415.99	196.69	2438.51	208.01
Paracentral	1635.95	235.37	1615.58	243.57	675.51	51.26	687.56	64.33
Frontal pole	472.20	72.05	482.30	76.55	160.92	17.71	160.80	19.86
Parietal								
Superior parietal	6626.01	840.76	6821.43	843.29	2183.66	203.79	2165.68	193.46
Inferior parietal	6193.94	859.28	6515.50	826.72	1887.03	182.54	1890.72	178.93
Supramarginal	4876.03	838.11	4436.49	882.30	1480.99	119.07	1466.08	121.88
Postcentral	5361.64	671.55	5181.26	608.15	2125.51	159.00	2130.29	173.24
Precuneus	4723.62	586.59	4790.12	619.13	1396.37	170.15	1409.70	182.28
Temporal								
Middle temporal	5036.97	683.12	5064.09	695.45	1459.38	172.32	1444.59	162.84
Inferior temporal	4974.64	710.57	4764.04	661.39	1277.37	152.59	1261.80	165.81
Superior temporal	4927.07	695.35	4827.50	599.52	1739.34	141.96	1679.95	126.64
Bankssts	1060.86	203.68	1110.63	202.06	180.74	19.72	183.66	23.04
Fusiform	4425.63	487.97	4425.54	476.65	1138.12	138.86	1128.37	180.16
Transverse temporal	546.02	119.69	503.17	90.96	148.72	19.02	145.65	17.73
Entorhinal	881.97	194.09	903.52	189.91	402.76	192.52	441.88	267.44
Temporal pole	873.88	111.82	815.78	101.82	333.26	54.69	325.25	45.87
Parahippocampal	1184.63	183.05	1185.68	205.07	588.51	251.39	614.45	347.94
Occipital								
Lateral occipital	5825.57	778.85	5920.21	864.59	2116.63	193.97	2172.38	260.93
Lingual	3754.40	476.37	3869.47	466.32	1302.34	254.80	1302.08	234.07
Cuneus	1813.12	220.92	1977.91	263.27	752.98	121.57	695.94	137.91
Pericalcarine	1472.42	288.75	1562.72	322.91	694.01	146.55	695.10	157.60
Cingulate & Insula								
Caudal anterior cingulate	979.53	220.59	1113.93	555.48	182.51	32.10	172.87	27.20
Isthmus cingulate	1477.15	508.80	1367.37	334.86	592.32	153.24	586.92	116.43
Posterior cingulate	1381.77	202.99	1439.18	276.60	481.14	52.23	479.08	57.70
Rostral anterior cingulate	1230.78	218.05	1261.12	583.52	491.07	157.80	462.00	214.64
Insula	2589.88	383.01	2636.68	447.67	1014.15	181.94	997.35	174.74

Table S1. Statistics of mean and standard deviation of regional surface area measurement for the human and chimpanzee brains.

Cortical Thickness	Human				Chimpanzee			
ROIs	Left Hemisphere		Right Hemisphere		Left Hemisphere		Right Hemisphere	
	mean	SD	mean	SD	mean	SD	mean	SD
Frontal								
Superior frontal	2.61	0.14	2.55	0.14	1.96	0.16	1.96	0.17
Rostral middle frontal	2.26	0.14	2.20	0.15	1.62	0.12	1.59	0.13
Caudal middle frontal	2.39	0.15	2.38	0.15	1.63	0.20	1.64	0.18
Pars-opercularis	2.48	0.14	2.47	0.15	1.72	0.16	1.72	0.17
Pars-triangularis	2.37	0.15	2.38	0.16	1.71	0.15	1.70	0.19
Pars-orbitalis	2.65	0.21	2.69	0.23	1.98	0.20	2.01	0.19
Lateral orbito frontal	2.57	0.16	2.55	0.17	2.02	0.15	2.04	0.15
Medial orbito frontal	2.27	0.18	2.27	0.16	1.65	0.18	1.66	0.17
Precentral	2.32	0.17	2.31	0.16	1.37	0.20	1.41	0.19
Paracentral	2.11	0.15	2.15	0.15	1.35	0.18	1.40	0.17
Frontal pole	2.79	0.29	2.73	0.28	1.77	0.25	1.77	0.22
Parietal								
Superior parietal	2.09	0.11	2.08	0.12	1.30	0.10	1.30	0.08
Inferior parietal	2.34	0.12	2.36	0.12	1.38	0.13	1.38	0.12

Supramarginal	2.49	0.13	2.48	0.14	1.58	0.14	1.56	0.14
Postcentral	1.98	0.10	1.96	0.12	1.23	0.09	1.23	0.09
Precuneus	2.27	0.14	2.27	0.12	1.35	0.13	1.31	0.12
Temporal								
Middle temporal	2.75	0.17	2.81	0.16	1.64	0.14	1.62	0.13
Inferior temporal	2.69	0.16	2.74	0.17	1.58	0.13	1.59	0.13
Superior temporal	2.68	0.15	2.72	0.15	1.45	0.15	1.46	0.14
Bankssts	2.44	0.16	2.51	0.19	1.37	0.19	1.36	0.18
Fusiform	2.56	0.18	2.58	0.16	1.33	0.10	1.34	0.11
Transverse temporal	2.32	0.20	2.33	0.19	1.24	0.19	1.28	0.17
Entorhinal	3.18	0.32	3.24	0.31	1.93	0.25	1.94	0.27
Temporal pole	3.61	0.27	3.63	0.30	2.15	0.26	2.16	0.26
Parahippocampal	2.45	0.22	2.50	0.20	1.23	0.16	1.28	0.17
Occipital								
Lateral occipital	2.13	0.12	2.18	0.13	1.19	0.09	1.21	0.07
Lingual	1.86	0.13	1.94	0.14	1.10	0.09	1.11	0.09
Cuneus	1.75	0.13	1.81	0.13	1.18	0.09	1.18	0.09
Pericalcarine	1.54	0.15	1.59	0.16	1.06	0.11	1.05	0.11
Cingulate & Insula								
Caudal anterior cingulate	2.27	0.27	2.24	0.23	1.39	0.20	1.31	0.18
Isthmus cingulate	2.16	0.19	2.16	0.17	1.44	0.15	1.47	0.13
Posterior cingulate	2.33	0.16	2.30	0.15	1.41	0.14	1.41	0.16
Rostral anterior cingulate	2.69	0.24	2.54	0.26	1.07	0.27	1.02	0.26
Insula	2.94	0.16	2.93	0.17	1.90	0.12	1.86	0.14

Table S2. Statistics of mean and standard deviation of regional cortical thickness measurement for the human and chimpanzee brains.

4 CT asymmetry computed based on FWHM filter sizes of 15, 10 and 5 mm

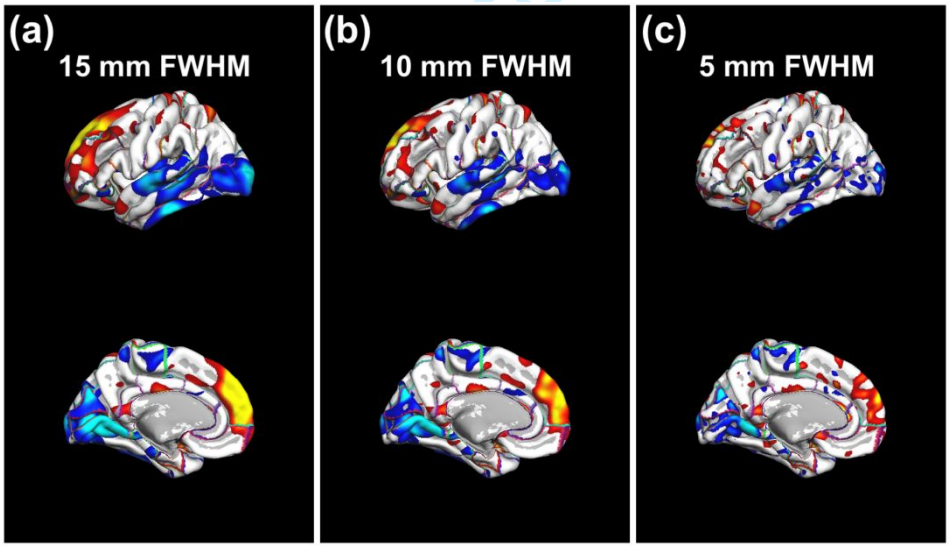

Figure S4. Significant CT asymmetry maps ($p<0.05$) computed with FWHM spatial filter size of (a) 15 mm, (b) 10 mm and (c) 5 mm showing (i) consistency in the asymmetry pattern for the human brain and (ii) 15 mm corresponds well with the size of brain petalia and gyri which are the features that are the focus of interest in the study. Hot colours refer to leftward asymmetry and cool colours to rightward asymmetry.